IDENTIFICATION OF ALLOSTERIC BINDING SITES OF THE ALLATOSTATIN RECEPTOR TYPE-C OF PINE PROCESSIONARY MOTH

by

Kübra Kahveci

B.S., Molecular Biology and Genetics, Yildiz Technical University, 2019

Submitted to the Institute for Graduate Studies in
Science and Engineering in partial fulfillment of
the requirements for the degree of
Master of Science

Graduate Program in Molecular Biology and Genetics
Boğaziçi University

2022

ACKNOWLEDGEMENTS

I want to express my gratitude to my supervisor, Assist. Prof. Necla Birgül. Thank you for your continued support and opportunities. Taking part in this beautiful project has given me a lot. I would like to thank her for always giving me faith, support, and guidance.

I thank my thesis defense committee, Prof. Serdar Durdağı, and Assist. Prof. Şükrü Anıl Doğan for sparing their precious time to evaluate my thesis and providing me with their invaluable feedback and thoughts. I would like to also thank Tübitak 119Z921 for funding this project.

I have to thank Alize Yılmazlar, Gökhan Gün, Barbaros Düzgün for their friendship and all former Cancer Signaling Laboratory (CSL) members, especially Aida Shahraki and Tolga Aslan, for teaching me a lot in such a short time. I will always be happy to be a member of CSL, and I am grateful to all the former and current CSL members for having their precious friendship.

I would like to express my sincere gratitude to Prof. Serdar Durdağı, head of the DurdağıLab where all the computational studies were performed. I will always feel grateful for welcoming me into his lab, never being able to thank him enough for the great opportunity he gave to me. During my DurdağıLab days, I learned a lot, which changed my perspective on my profession. I am also grateful to all DurdağıLab members, which have been a family to me, and I will never forget what great friends they are.

I want to thank my dearest friends with whom I lived my MSc. adventure, Alize Yılmazlar, Özlem Kartal and Selmanur Keskin. Also, I want to thank the Molecular Biology and Genetics Department for their continued support.

I will forever appreciate my dear family for always trusting, supporting, and

believing in me. They have always been there for me to make my dreams come true. No matter how far we are, I am grateful to my dear friends, who always support me and make me feel their love. Whenever I fell into darkness, they were there to hold my hand. Without their support, life would be an unbearable place.

ABSTRACT

IDENTIFICATION OF ALLOSTERIC BINDING SITES OF THE ALLATOSTATIN RECEPTOR TYPE-C OF PINE PROCESSIONARY MOTH

G-protein coupled receptors (GPCRs) are cell surface receptors that are consisted of seven-transmembrane α helices. Drugs targeting GPCRs account for one-third of clinically approved drugs; since many drugs target the conserved orthosteric site, they result in side effects like chronic administration, drug resistance, and desensitization. Allosteric sites are topographically distinct from the orthosteric site. Allosteric modulators modulate the binding and signaling properties of the orthosteric site and orthosteric ligands, fine-tune receptor signaling, reduce the risk of overdosing, and increase specificity since they bind to structurally less conserved sites. Insect GPCRs are a potential target for developing pest control agents as many of these receptors regulate different physiological functions in insects. C-type Allatostatin Receptor (AstR-C) is a class A GPCR and regulates a vital pathway, Juvenile Hormone synthesis, presenting a potential pesticide target. *Thaumetopoea pityocampa* is the main factor that limits the development and survival of the Mediterranean pine forests. The study aims to provide a safer pesticide with efficient functionality by utilizing *in silico* and *in vitro* methods to identify allosteric binding pockets and find allosteric modulators of AstR-C. Various allosteric site prediction tools and blind-docking methods were employed to identify allosteric binding sites. Virtual screening was applied to three potential sites, and hit molecules were subjected to MD simulations and MM-GBSA analysis. Two potential allosteric sites were detected in transmembrane (TM) domains 4, 5, and ECL-2. A third pocket was determined between TM 3-4 and ICL-2. A total of 5 molecules, two molecules for each binding site, yielded promising results in the analyses.

ÖZET

ÇAM KESE BÖCEĞİNİN ALLATOSTATİN C-TİPİ RESEPTÖRÜNÜN ALLOSTERİK BAĞLANMA CEPLERİNİN BELİRLENMESİ

G-proteinine bağlı reseptörler (GPCR'ler), yedi transmembran alfa sarmaldan oluşan hücre yüzeyi reseptörleridir. GPCR'leri hedefleyen ilaçlar, klinik olarak onaylanmış ilaçların üçte birini oluşturmaktadır ve birçoğu korunmuş ortosterik bölgeyi hedef aldığından, kronik uygulama, ilaç direnci ve duyarsızlaşma gibi yan etkilere neden olurlar. Allosterik cepler topografik olarak ortosterik bölgeden farklıdır. Allosterik modülatörler, ortosterik bölgenin ve ligandlarının bağlanma ve sinyal özelliklerininde ince ayar yapabilir, aşırı doz riskini azaltabilir ve daha az korunmuş ceplere bağlanarak spesifikliği arttırabilirler. Böcek GPCR'lerin birçoğu böceklerde farklı fizyolojik fonksiyonları düzenler. Bu sebeple haşere kontrol ajanları geliştirmek için potansiyel hedeflerdir. C-tipi Allatostatin Reseptörü (AstR-C), A sınıfı bir GPCR'dir ve böcekler için hayati önem taşıyan Juvenil Hormon sentezini düzenlediğinden potansiyel bir pestisit hedefi sunar. *Thaumetopoea pityocampa*, Akdeniz çam ormanlarının gelişimini ve hayatta kalmasını ana tehdittir. Bu çalışma ile AstR-C'nin allosterik bağlanma ceplerini tanımlamak ve allosterik modülatörlerini bulmak, *in silico* ve *in vitro* yöntemler kullanarak verimli, işlevsel, ve daha güvenli bir pestisit sağlamayı amaçlanmaktadır. Allosterik bağlanma bölgelerini belirlemek için çeşitli allosterik paket tahmin araçları ve kör yerleştirme yöntemleri kullanıldı. Üç potansiyel bölgeye sanal tarama uygulandı ve uygun moleküller moleküler dinamik simülasyonlarına ve MM-GBSA analizine tabi tutuldu. Transmembran (TM) alanları 4, 5 ve ECL-2'de iki potansiyel allosterik bölge tespit edildi. TM 3-4 ve ICL-2 arasında üçüncü bir cep belirlendi. Her bağlanma bölgesi için iki molekül olmak üzere toplam 5 molekül, analizlerde umut verici sonuçlar verdi.

TABLE OF CONTENTS

LIST OF FIGURES

LIST OF TABLES

LIST OF SYMBOLS

g	Gram
l	Liter
M	Molar
m	Meter
n	Nano
α	Alpha
Å	Angstrom
β	Beta
Δ	Delta
δ	Delta
γ	Gamma
κ	Kappa
μ	Mu
τ	Tau

LIST OF ACRONYMS/ABBREVIATIONS

2D	Two Dimensional
3D	Three Dimensional
7TM	7-Transmembrane
AST	Allatostatin
AstR-C	Allatostatin Receptor Type C
BRET	Bioluminescence Resonance Energy Transfer
BSA	Bovine Serum Albumin
Cα	Carbon Alpha
CA	Corpus Allatum
cAMP	Cyclic Adenosine Monophosphate
CC	Corpus Cardiacum
CO_2	Carbon Dioxide
cryo-EM	Cryo-Electron Microscopy
C-terminus	C-terminal Loop
ddH_2O	Double Distilled Water
DMEM	Dulbecco's Modified Eagle Medium
DNA	Deoxyribonucleic Acid
ECL	Extracellular Loop
EDTA	Ethylenediaminetetraacetic Acid
EtBr	Ethidium Bromide
EtOH	Ethanol
FAO	Food and Agriculture Organization
FBS	Fetal Bovine Serum
FRET	Fluorescence resonance energy transfer
GDP	Guanosine Diphosphate
GIRK	G Protein-Coupled Inwardly Rectifying Potassium Channel
GPCR	G Protein-Coupled Receptor
GRK	G Protein Receptor Kinase
GTP	Guanosine 5'-triphosphate

HCl	Hydrochloric Acid
ICL	Intracellular Loop
IM	Intermediate
JH	Juvenile Hormone
$MgCl_2$	Magnesium Chloride
MD	Molecular Dynamics
min	Minutes
mRNA	Messenger Ribonucleic Acid
NaCl	Sodium Chloride
NaOAc	Sodium Acetate
NaOH	Sodium Hydroxide
NCBI	National Center for Biotechnology Information
ns	Nanosecond
N-terminus	N-terminal Loop
OD	Optical Density
OPM	Orientation of Protein in Membrane
PBS	Phosphate Buffered Saline
PDB	Protein Data Bank
rcf(g)	Relative centrifugal force
RMSD	Root Mean Square Deviation
RMSF	Root Mean Square Fluctuation
RNA	Ribonucleic Acid
RT	Room Temperature
SD	Standard Deviation
SDM	Site-Directed Mutagenesis
sec	Seconds
SEM	Standar Error of the Mean
TpitAstRC	Allatostatin Receptor Type C of Pine Processionary Moth
TM	Trans-membrane

1. INTRODUCTION

1.1. G-protein Coupled Receptors

G-protein coupled receptors (GPCRs) are cell surface receptors that are consisted of seven-transmembrane α helices, three extracellular (ECL), and three intracellular loops (ICL) [1]. The N-terminal domain is localized at the extracellular site, while the C-terminal domain is localized at the intracellular site [2]. GPCRs can be stimulated by various ligands, e.g., peptides, odorants, hormones, ions, and even photons [3]. These receptors are classified into six families based on amino acid sequence and functional roles [4]. Class A is the most prominent family of GPCRs known as "rhodopsin-like" receptors [5]. Since it contains neurotransmitter receptors to light receptors, it is a pretty diverse family of proteins [6]. The secretin-like family (Class B GPCRs) includes 15 peptide hormone receptors that have roles in many metabolic and neurological pathways, which makes Class B GPCRs a popular drug target, notwithstanding that it is a small family [7]. Class C GPCRs are characterized by dimerization and their long N-terminal domain, which obtains the orthosteric binding pocket. Metabotropic glutamate receptors (mGlu), γ-aminobutyric acid B receptors (GABAB), calcium, and taste receptors are the members of Class C [8, 9]. Class D receptors, also known as fungal pheromone P-, α-factor receptors, are extensively expressed in fungi. These receptors regulate the fungi metabolism, reproduction, development, and survival of fungi species [10]. For these reasons, they are a potential target to treat fungi infections. Fungal pheromone A- and M-factor and cAMP receptors are classified as Class E GPCRs [11]. Lastly, Class F contains 10 frizzled (FZD) receptor subtypes and smoothened (SMO) receptors which have roles in embryonic development during cell migration, differentiation, cancer progression, and cell homeostasis [12–14].

1.2. Structural Characteristics of Class A GPCRs

GPCRs share sequence identity with the family members [15]. Especially in the transmembrane regions, the amino acid sequence is highly conserved among the

GPCRs [16, 17]. They usually show differences in the loop, N- and C-terminal regions, which are diverse in length and sequence [18]. ICL-2 and ICL-3 are mostly related to G-protein binding, and variety in the length of ICL-3 is associated with G-protein selectivity [19]. It is also shown that ICL-2 structure is important for receptors to achieve active conformation [20]. Whereas ECL-2 is mostly associated with ligand binding, specificity, and activation initiation [21]. Although there is diversity, there are also shared structural and functional properties among the GPCR A family, especially in the activation mechanism and its components which are referred to as motifs [22]. The Ballesteros-Weinstein nomenclature system is often used to indicate GPCR residues based on their location and conservation [23]. The first number shows the transmembrane helix, and the second shows the position of the residue compared to the most conserved residue, which is numbered 50. The number increases towards to N-terminal, and it decreases towards to C-terminal. This numbering system will refer to the residue locations in this document.

The ionic lock is one of the most important control mechanisms for GPCR activation [24]. It stabilizes the inactive conformation, and disruption of the ionic lock induces GPCR activation [25]. Ionic lock is an interplay between $Arg^{3.50}$ of (D/E)RY motif and adjacent $D/E^{3.49}$ and $D/E^{6.30}$ of TM6 which are located at the cytosolic part. A positively charged side chain of arginine and negatively charged side chain of aspartate interact through the ionic bond [26]. $Arg^{3.50}$ is also a part of the hydrophobic arginine cage, which restrains the movement of receptors in the inactive state through interactions with the hydrophobic residues located at 3.46 and 6.37 positions [27]. CWxP motif ($C^{6.47}$, $W^{6.48}$, $P^{6.50}$) is a highly conserved micro-domain and functions as rotamer toggle switch in GPCR activation [28]. Proline residue is present in 98% of sequences, and the side-chain of Proline creates a kink in the α helices, which can mediate the movement of TM6 lower half [29]. The rotameric switch of $W^{6.48}$ is accompanied with side-chain rotations of $C^{6.47}$ and $F^{6.52}$. The outward movement of TM6 leads the receptor activation, creating an opening for the G-protein binding [30, 31]. Na^+ ion has a negative allosteric effect and is also observed in crystal structures of A_{2A}AR accompanied by water molecules [32]. Na^+ pocket is consisted of $D^{2.50}$, $S^{3.39}$, $C^{6.47}$, $N^{7.45}$, and $N^{7.49}$ [33]. Ligand stimulation initiates conformational rearrangements

and Na^+ pocket collapses which trigger TM6 outward movement [34]. $P^{5.50}$ $I^{3.40}$ $F^{6.44}$ motif is mostly positioned under the orthosteric pocket [35]. Upon ligand binding, orthosteric pocket contracts and leads to conformational changes in Na^+ pocket and PIF motif [36]. $N^{7.49}$ $P^{7.50}$xx$Y^{7.53}$ motif stabilizes active conformation of the receptor by enhancing packing of TM3 and TM7 [37].

1.3. Structural Basis of GPCR Activation

A common activation pathway for Class A GPCRs has been defined. The allosteric network of GPCRs transmits the signal from the orthosteric pocket to G-protein binding site with conserved micro-domains, connecting the extracellular and intracellular sides of the receptor [38]. Upon an activation ligand binding, the rotameric switch of $W^{6.48}$ is activated, and the side chain of $F^{6.44}$ rotates [39]. A rearrangement occurs in the PIF motif, and Na^+ pocket collapses [36]. The collapse of Na^+ pocket leads to denser packing of TM7 with TM3 [40]. $Y^{7.53}$ of NPxxY forms new contacts with $L^{3.43}$ $I^{3.46}$ $R^{3.50}$ residues [41]. Salt bridge between residues $Arg^{3.50}$ and $D/E^{6.30}$ are eliminated, accompanying receptor activation, and this motion release the intracellular end of TM6 from TM3, which results in activation hallmark, the outward movement of TM6 [42]. Receptor activation opens a pocket with TM7-TM3 packing and TM6-TM5 movement in the cytoplasmic side of the receptor for the Gα-coupling, and $Arg^{3.50}$ along with 3.53, 3.54, 5.61 and 6.33 residues makes contact with Gα to further stabilize active conformation [43].

1.4. GPCR Signaling

GPCRs recruit heterotrimeric G-protein following receptor activation to initiate downstream signaling pathways [44]. Heterotrimeric G-proteins are Gα, Gβ, Gγ, further divided into subtypes. 21 Gα subunits encoded by 16 genes, 6 Gβ subunits encoded by 5 genes, and 13 Gγ subunits encoded by 13 genes in humans. Gα subunits are grouped into four main classes according to sequence similarity: Gαs (Gα_s, Gα_{olf}), Gα_i (Gα_t,Gα_{i1}, Gα_{i2}, Gα_{i3}, Gα_{o1}, Gα_{o2}, Gα_z), G$\alpha_{q/11}$ (Gα_q, Gα_{11}, Gα_{14}, Gα_{15}, Gα_{16}), and Gα_{12}, (Gα_{12}, Gα_{13}) [45]. Gα dissociates from the heterotrimeric complex in recep-

tor activation while G$\beta\gamma$ dimer remains [46]. Gγ subunits have more variation in the case of sequence and tissue expression, although subunits of Gβ show high sequence similarity. Thus, the functional specificity of the G$\beta\gamma$ dimer is affiliated to γ [47]. The α-helical domain (AHD) and the Ras-like (Ras) GTPase domain are important functional hotspots of Gα for nucleotide exchange during activation. Loops of the Ras domain take a role in guanosine diphosphate (GDP) binding. AHD inserts bound nucleotide to the interface located between AHD and Ras domain [48].

β-arrestins can initiate GPCR-related signaling cascades through G-protein independent pathways [49]. The nonvisual arrestins are β-arrestin 1 (β-arrestin 2) and 2 (also known as β-arrestin 3). β-arrestin (βarr) recruitment can mediate receptor desensitization, endocytosis, and distinct signaling pathways [50]. Phosphorylation by GPCR Kinase (GRK) of the C-terminus of the receptor, in some cases, involves some intracellular loops, too, leading to interaction with a positively charged groove within the N-terminus domain of βarr [51]. The C-terminus tail of β-arr acts as an autoinhibition mechanism for β-arr. Receptor engagement requires displacement of the β-arr C-tail from the N-domain groove and agonist-bound receptor. Phosphorylated receptor C-tail and agonist bound-receptor trigger β-arr C-tail removal from the N domain and lead to β-arr coupling [52].

After Gα dissociation in receptor activation, G$\beta\gamma$ activates GRKs by binding to the pleckstrin homology (PH) domain to shut off signaling of the GPCR [53]. GRK activation is dependent on G-protein activation. However, it has been reported that the Dopamine receptor (D2R) can recruit GRK2 without G-protein activation [54]. GRK phosphorylation is important for β-arr mediated signaling since the phosphorylation sites functions as a barcoding system to recruit specific β-arr conformations and functions. It is named phospho-barcode theory and is essential for β-arr biased signaling in GPCRs [55].

In Figure 1.1, various outcomes of GPCR activation were represented. When GPCR is activated by a ligand, it initiates GDP dissociation from G$\alpha\beta\gamma$. Since guanosine triphosphate (GTP) concentration is high in cells, Gα binds GTP to its nucleotide

binding site in a short time, and Gα dissociates from the G$\beta\gamma$. G-protein coupling can mediate different signaling cascades by affecting adenylyl cyclase, cGMP phosphodiesterase, phospholipase C and RhoGEF proteins and transmit signals through second messengers. When Gα hydrolysis GTP via its GTPase activity, GDP-bound Gα reconnects with G$\beta\gamma$ dimer. On the other hand, G$\beta\gamma$ can activate GRKs to the membrane for GRK-mediated phosphorylation of the receptor, which can result in desensitization, trafficking between potassium channels and kinases, or inducing distinct signaling cascades. Receptor internalization occurs via clathrin-coated endocytosis, which may result in degradation, recycling, or intracellular activation of the receptor [42, 56, 57].

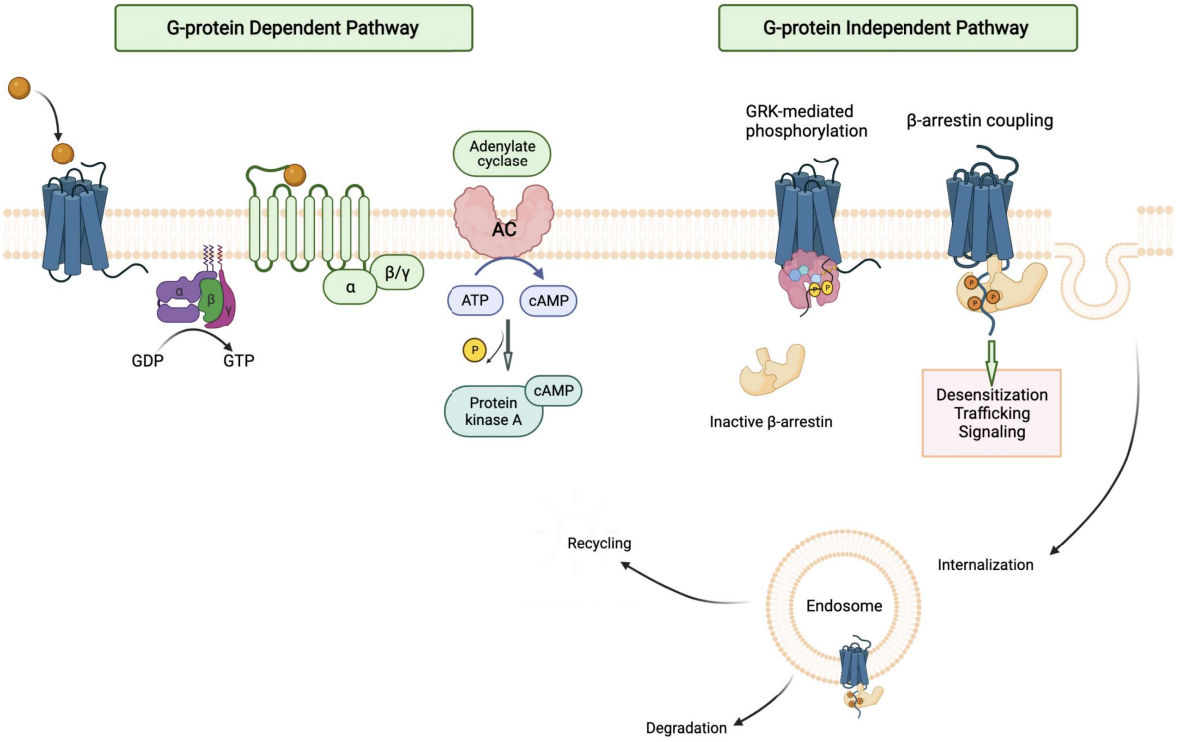

Figure 1.1. GPCR signaling pathways.

1.5. Allosteric Modulation

Allostery is the regulation of a protein function via the binding of a modulator to a topographically distinct site from an orthosteric pocket [58]. The allosteric signal is transmitted across the protein structure via conformational changes, atomic fluctuations, and amino acid motif networks [59]. Fine-tuning receptor signaling, en-

hancing ligand affinity, further stabilizing certain conformations, increased specificity, reduced side effects, and toxicity makes the allostery concept attractive for therapeutic investigations [60].

Monod-Wyman-Changeux (MWC) was the first model that explained allostery [61]. Early models tend to describe two major conformational states for protein structure, and the MWC model assumes that protein domains are in the same conformational state. Therefore, conformational changes occur all-or-none fashion and shift the equilibrium into a high-affinity state and result in cooperative ligand binding [62]. Koshland–Nemethy–Filmer (KNF) Model explains the allosteric effect in sequential steps and induced fit mechanism. Ligand binding to a domain initiates conformation changes in another domain, thus indicating a presence of an interdomain signal [63]. The population shift model extended previous models into a free energy landscape model. It assumes that a protein in apo form exists in multiple conformations. By a ligand binding to the most appropriate conformation, it shifts the population of conformations to the conformation favored by the effector ligand [64, 65].

Allosteric Ternary Complex Model (ATCM) was the first model to explain the allosteric effect between GPCR and G-protein, and it is described as a mechanistic model [66]. It was directly usable in experiments if the allosteric ligand changes the affinity of the orthosteric ligand. However, it is limited since it does not explain the isomerization between active and inactive states of the receptor [67]. Additionally, although it can show the allosteric effect on orthosteric ligand affinity, it cannot explain the other allosteric effects on orthosteric ligand signaling efficacy. Extension of this model was presented with the Allosteric Two State Model (ATSM), which includes the active-inactive state isomerization of the receptor and explains selective stabilization of the conformation by orthosteric and allosteric ligands [68, 69]. The operational model was originally proposed to explain agonism by Black and Leff, [70] and extended further by Leach and Kenakin [71] explain allosterism and biased modulation. Quantifying efficacy among different systems is hard since the response to the effector can vary in distinct systems. The operational model includes operational efficacy parameters, thus, presenting an applicable tool for different systems to evaluate agonism, allostery,

and bias [72, 73].

With the research in the field of allostery, it has been seen that GPCRs do not work as simple on-off mechanisms and operate in a much more complex structure [30]. To further understand the concept of allostery, allosteric ligands, and biased modulation should be explained. Positive allosteric modulators (PAM) increase the functional response of an orthosteric ligand, whereas negative allosteric modulators (NAM) show inhibiting activities. There are also neutral allosteric ligands (NAL), also known as silent allosteric modulators (SAM), that do not affect receptor activity but compete with other allosteric ligands [74]. Additionally, it has been reported that some allosteric ligands can activate or inhibit the receptor depending on the cellular composition despite binding the allosteric pockets, and they are called PAM-agonists (ago-PAM) and NAM-agonists [75]. On the other hand, bitopic ligands own orthosteric and allosteric functional parts that can engage with the receptor [76]. A biased ligand can selectively activate signaling pathways while blocking another. In the case of GPCRs, they can selectively activate G-protein-dependent pathways while blocking β-arr signaling or vice versa [77].

1.6. Pharmacological Attributes of GPCR Allostery

There are five properties of GPCR allostery which are ceiling effect, probe dependence, subtype selectivity, biased modulation, and oligomerization [78]. The ceiling effect or saturability effect is explained as after a certain concentration of the allosteric ligand, the modulation effect is saturated. After the highest concentration possible for allosteric modulation, it reaches its limit and maintains the orthosteric ligand signaling while no additional modulation above the "ceiling" will not be observed [79]. Saturation of the allosteric effect provides the fine-tuning of the receptor signaling and reduces the risk of overdosing [80].

Probe dependence is the mediation of the allosteric ligand effect by the orthosteric ligand [81]. Direction and the extent of the allosteric effect are dependent on the orthosteric ligand. Therefore, one allosteric modulator can show different effects with

different orthosteric ligands on the same receptor [82]. Even with the same allosteric modulator-orthosteric ligand-receptor combination, the allosteric effect can change in different organisms because the cooperativity with the orthosteric ligand and model organism can differ [83]. Thus, it can be stated that PAM, NAM, or SAM categorization is context-dependent, and it is linked to receptor conformational state and cellular context [84].

The orthosteric binding site is highly conserved among the GPCRs, and it is even higher in receptor subtypes which makes it harder to selectively target the receptors without causing off-target side effects [3]. Allosteric pockets are less conserved and quite diverse in sequence identity, although interestingly, allosteric sites are similar structurally based on the crystal structure data. Thus, allosteric modulators provide receptor selectivity on related subtypes and provide cooperativity with the orthosteric ligand that binds to that particular receptor [85, 86].

Allosteric ligands can favor one signaling pathway over another by stabilizing the receptor conformation associated with the downstream pathway [87, 88]. It provides the potential to target the desired therapeutic pathway via their interaction with the orthosteric ligand [89, 90].

Although there is still some controversy about allostery in oligomeric structures of GPCRs, it has been reported in several experimental studies [91–94]. According to the experimental results, allosteric interaction can be observed between oligomeric GPCRs [95].

1.7. Advantages and Challenges in Allosteric Drug Discovery

Drugs targeting GPCRs account for one-third of clinically approved drugs [96]. According to GPCRdb, 94% of these drugs are targeted to the Rhodopsin family of GPCRs, and 92% of them are small molecules [97]. A small fraction of them forms allosteric molecules, and allosteric drugs targeting GPCRs are listed in Table 1.1. Since many drugs target the conserved orthosteric site, the selectivity is reduced, side effects

are seen in receptor subtypes, and closely related families are also affected [98]. Moreover, chronic administration, drug resistance, and desensitization due to prolonged exposure cause a lack of efficacy for these molecules [99]. Thus, allosteric molecules have great potential to improve chemical and physiological research and can afford numerous advantages [100].

Table 1.1. Clinically tested allosteric drugs targeting GPCRs.

Drug Name	Indication	Receptor Family	Status	Phase	Drug Type	Mechanism
adx71441	Neurologic disorders	GABAB receptors	preclinical	0	small molecule	PAM
adx71441	Neurologic disorders	GABAB receptors	preclinical	0	small molecule	PAM
adx-71149	Antipsychotic; Anti-depressant; anxiolytic	Metabotropic glutamate receptors	in trial	2	small molecule	PAM
akp-11	Psoriasis	Lysophospholipid (S1P) receptors	in trial	1	small molecule	PAM
ap1030	Anti-obesity	Melanocortin receptors	in trial	1	small molecule	PAM
ap1030	Anti-obesity	Melanocortin receptors	in trial	1	small molecule	PAM
pxt002331	Antiparkinson	Metabotropic glutamate receptors	in trial	1	small molecule	PAM
cinacalcet	Hyperparathyroidism	Calcium-sensing receptors	approved	4	small molecule	PAM
cinacalcet	Calcimimetics	Calcium-sensing receptors	approved	4	small molecule	PAM
etomitate	Anesthetics; Intravenous	Adrenoceptors	approved	4	small molecule	PAM
ticagrelor	antithrombotic	P2Y receptors	approved	4	small molecule	NAM
adx415	Antihypertensive	Adrenoceptors	in trial	2	small molecule	NAM
adx-48621	Antiparkinson	Metabotropic glutamate receptors	in trial	2	small molecule	NAM
basimglurant	Fragile X syndrome	Metabotropic glutamate receptors	in trial	2	small molecule	NAM
dipraglurant	Antiparkinson	Metabotropic glutamate receptors	in trial	2	small molecule	NAM
stx107	Fragile X syndrome	Metabotropic glutamate receptors	in trial	2	small molecule	NAM
adx10059	Anti-migraine; gastroesophageal reflux disease	Metabotropic glutamate receptors	discontinued	2	small molecule	NAM
decoglurant	Unipolar depression	Metabotropic glutamate receptors	discontinued	2	small molecule	NAM
decoglurant	Unipolar depression	Metabotropic glutamate receptors	discontinued	2	small molecule	NAM
namacizumab	Fibrosis	Cannabinoid receptors	in trial	1	antibody	NAM

The greatest challenge in targeting GPCRs is selectivity. It has been observed that orthosteric ligands usually suffer from cross-reactivity between related receptor families and result in side effects and toxicity [101]. Furthermore, allosteric ligands present their activity by fine-tuning the orthosteric ligand signaling rather than completely switching on or off the receptor signaling. These feature helps to prevent overdosing and provide safety for allosteric molecule usage. Allosteric modulators can help to manage drug resistance rooted in orthosteric site mutations, as asciminib helps to overcome the drug resistance that T315I causes in the BCR-ABL kinase receptor [102]. GPCRs are highly dynamic proteins and exist in multiple conformations, which gives them the ability of involved in different signaling pathways. An allosteric modulator can bind to a specific conformation of the receptor that favors G-protein or β-arr signaling, and achieved receptor-ligand conformation can activate these pathways [103].

Allosteric modulators have proven that formerly believed undruggable targets can be treated like in the examples of K-Ras, STAT3, and MYC [104].

Allosteric and orthosteric ligands stabilize the receptor's conformation after binding to their respective sites [105]. In another case, they shift the equilibrium of the receptor population to the favored one from the effector. In the case of PAMs, they shift the inactive population to the active one. However, the shift in the equilibrium by an allosteric ligand is quite small, so it is not easily detected in GPCR signaling assays [106]. An orthosteric ligand binding can further stabilize the conformation triggered by the allosteric modulator [107]. Amplifying receptor expression can help increase stimuli-receptor response. Even so, it is harder to discriminate the allosteric effect from the orthosteric ligand efficacy. Thus, GPCRs should be considered as a structure consisting of allosteric microdomains that can form many conformations as a response to distinct ligands [108]. Therefore, allosteric ligand discovery promises new opportunities as well as challenges to overcome.

Research in the field of allosteric modulator discovery has shown that these molecules have different physicochemical properties compared to orthosteric ligands. Allosteric modulators have exhibited high lipophilicity, and rigidity [109]. Also, problems in structure-active relationships such as low affinity to their respective binding site and complexities in incorporating polar and soluble groups demand more molecular characterization [104]. Less conservation of allosteric sites can cause the problem of less efficacy between species. Furthermore, evolutionary less conservation of allosteric sites makes it challenging to identify them [110]. Mutations in the allosteric pockets can generate resistance to the allosteric modulator and change the receptor response to the orthosteric-allosteric ligand combination. Besides the allosteric site mutations, abnormalities in the allosteric network can affect the allosteric modulation [104]. Allosteric modulators' state dependence could give rise to an obstacle in degenerative diseases with changing endogenous orthosteric tone. If functional bias is not considered when allosteric modulator design, it may result in unforeseen effects on cell physiology [111]. On the other hand, thanks to developments in experimental and computational approaches, steps have been taken to overcome these problems.

1.8. Methods to Investigate GPCR Allostery

X-ray crystallography and cryo-EM methods have played a major role in determining the structures of difficult-to-image molecules such as GPCR [46, 112]. The identification of 3D structures facilitates the identification of allosteric packages [98]. However, since X-ray crystallography and cryo-EM are snapshots of the static structures of molecules, they are not sufficient to detect small conformational changes caused by allostery. At this point, NMR spectrometry allows dynamically monitoring the changes in molecules with durations such as ps-ms, which is very suitable for observing the allostery mechanism [99]. Site-directed mutagenesis can help to verify predicted allosteric sites [113]. Fluorescence resonance energy transfer (FRET), bioluminescence resonance energy transfer (BRET), cAMP accumulation, Ca^{+} flux, β-arr recruitment, and TANGO assays can give insights into the allosteric modulator-receptor interactions [42, 114–119]. However, such experimental methods need alternative methods as they take a lot of time and are not always sufficient to determine complex allosteric mechanisms.

Computer-based methods are emerging as a powerful tool for allosteric drug discovery, saving time and cost. Developing and constantly updating databases such as AlloStericDatabase (ASD) and ASBench increase the efficiency of *in-silico* studies [120, 121]. Many tools were developed based on different methods for allosteric pocket determination, which is the first step in allosteric drug design [122]. These are structure, evolution, normal model analysis, dynamics, molecular dynamics (MD) simulations with enhanced conformational sampling, perturbation, and correlation-based methods [123–125]. Virtual-screening methods in finding allosteric modulators save time for experimental studies by scanning very large ligand libraries in a short time and reduce the cost by greatly reducing the number of molecules to be tested [126]. MD simulations support studies by providing data on the different conformations of GPCRs [37]. It can give insight into the dynamic nature of the GPCRs [127]. However, computer-based methods require serious computer resources. The combination of experimental and computer-based methods has the potential for success in allostery research by supporting each other's shortcomings while benefiting from the advantages

of both methods.

1.9. Pesticides

Food and Agriculture Organization (FAO) define pests as species harmful to plants and their products, vectors of pathogens, and parasites that cause illness in humans or other animals. Minor pests contribute to a 5–10% damage rate, whereas major pests contribute to higher than 10% [128]. Pesticides are substances that target pest organisms to prevent outbreaks and damages, and they have been conventionally used by humans since the first times of civilization [129].

Pesticides can be classified differently based on their chemical structure, target organism, mode of action, and toxicity. Classification according to the chemistry results in groups of organochlorines, organophosphorus, and inorganic. Organochlorines tend to disrupt neurological systems and result in insects' death by causing convulsions and paralysis. Organophosphorous molecules cause a malfunction in neural synapses by inhibiting the neural impulses, which leads to rapid twitching in muscles, paralysis, and death. On the other hand, inorganic substances generally induce stomach poisoning [130]. In Figure 1.2, insecticides were grouped based on physiological targets.

With the invention of dichloro-diphenyltrichloroacetic acid (DDT), pesticide usage was increased due to a significant increase in crop yield. These chemicals were affordable and effective in a large span of insect species. With the success of DDT, more and more effective pesticides have been produced [131]. However, it was later realized that the effectiveness of these chemicals was escalated because they were extremely toxic. This situation aroused awareness about pesticides, and institutions such as the insecticide resistance action committee (IRAC) emerged, which are still active today.

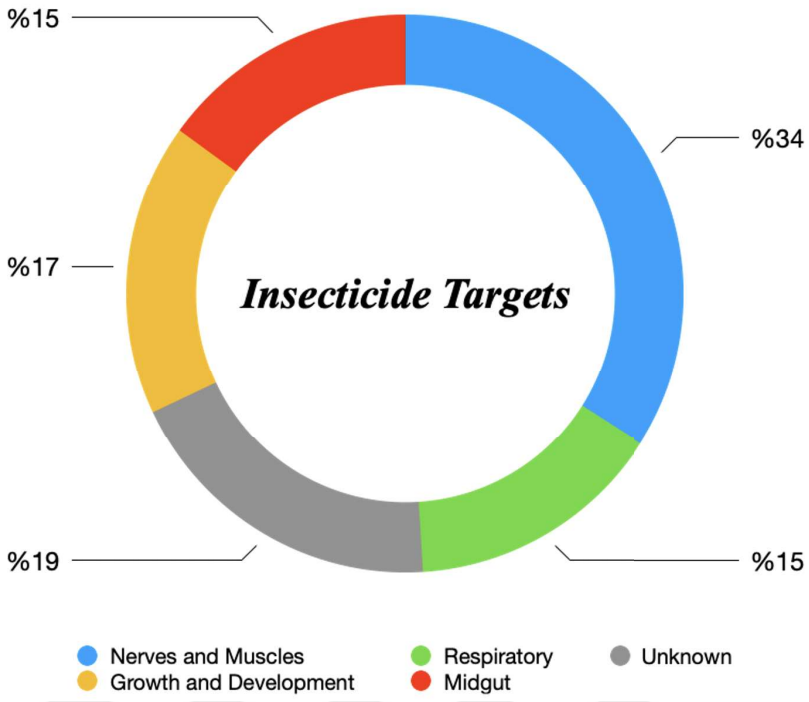

Figure 1.2. Physiological targets of insecticides.

1.9.1. Benefits and Hazards

Pesticides provide safety from pests to increase agricultural productivity by improving crop yield and quality. The amelioration in agriculture engenders economical opportunities to provide affordable food and high profits for farmers [132]. Producing quality and safe food available to everyone will improve nutrition and help improve quality of life and prolong life [133]. Prevention of vector-borne diseases such as malaria and sleeping sickness will preclude large-scale outbreaks of epidemic diseases [134]. Pesticides can restrict diseases in a small area by discarding pathogen hosts [135]. Gardens, landscapes, wooden structures, paintings, and buildings are prone to pest invasion and can be protected by pesticides. Besides nutrition, crops are used as renewable fuels and chemical feedstocks, which is another economical benefit of pesticide protection. Furthermore, transportation systems are also protected with pesticides by eliminating unwanted roadway plants [136, 137].

Extensive and improper pesticide usage gave rise to new environmental toxic-

ity and bioaccumulation [138]. False application and spraying equipment and poor storage techniques led to soil, water, and food contamination which are threatening public health and non-target organisms [139, 140]. Soil contamination causes groundwater contamination and pollutes the aquatic environment, which increases the risk of contaminated drinking water [141]. Chronic exposure to pesticides via inhalation, ingestion, or dermal contact can trigger serious health problems [142–144]. Increased reactive oxygen species (ROS) levels, inflammatory diseases, and neurological disorders, especially Parkinson's disease, have been reported as a result of exposure to pesticides by various studies [145, 146]. Imbalance in ROS levels is associated with defects in cell homeostasis and DNA stability [147–149]. Besides genotoxicity, carcinogenic risks are also reported [150, 151]. Moreover, to environmental and public health distress, many pest species have developed resistance due to incorrect usage of pesticides [152–154].

There is a dilemma in pesticide usage due to its benefits and certain risk factors. However, counterbalancing the drawbacks with increased selectivity and target specificity of the chemicals is possible. It shows that there is a demand for next-generation pesticides that can provide more target-specificity with minimized side effects.

1.9.2. Next-Generation Pesticides

Conventionally used pesticides gave rise to resistance development and environmental hazards, creating an urgent need for novel pesticides [155]. To overcome these obstacles, various approaches were implemented, which are using some organisms like bacteria, fungi, nematodes, etc., as biological agents, essential oils, secondary metabolites, RNA interference (RNAi), and Juvenile Hormone (JH) mimics, and peptides [156, 157]. Essential oils are extracted from plants, and they have insecticide, insect repellent, nematicide, and acaricide properties. They show their lethal effects by neurotoxicity via inhibiting acetylcholinesterase, octopamine receptors, and GABA receptors. But due to their volatility and low bioavailability, wide-scale usage is not pragmatic [158]. RNAi provocation in insects can lead to growth inhibition, reduced fertility, developmental anomalies, and mortality [159]. RNAi's most prominent aspect is its potential for high target selectivity due to its sequence-specific nature. [160]

Oral uptake, microinjection, or unstable/transient expression in transgenic plants are the possible delivery methods. Environmental stability and concentration must be addressed to make it suitable for commercial applications [161]. JH mimics are also ideal pest management agents since this hormone affects the insect life cycle like metamorphosis, reproduction, and development [162]. JH mimics are also ideal pest management agents since this hormone affects the insect life cycle like metamorphosis, reproduction, and development. Disruption of the JH balance results in defects in the nervous and muscular systems and abdominal differentiation [163, 164].

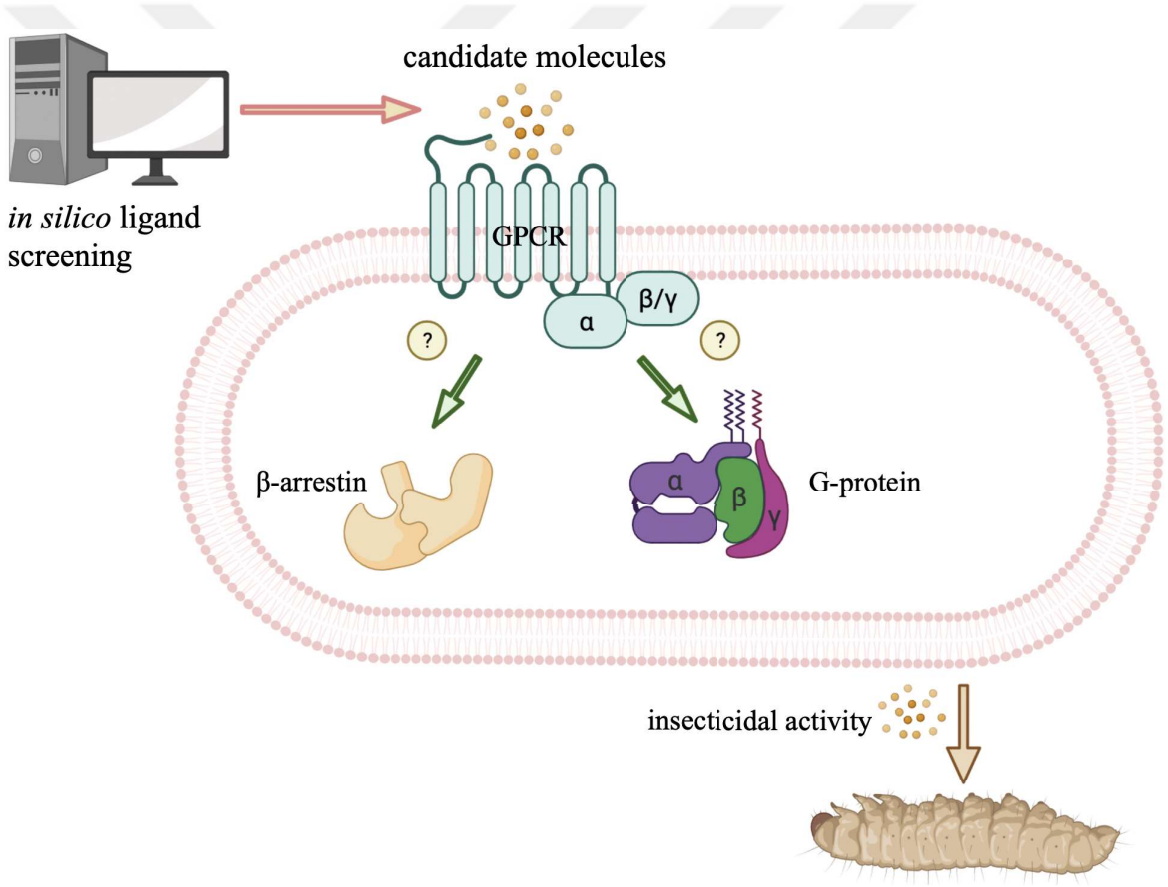

Figure 1.3. GPCRs as next-generation pesticides targets.

Neuropeptides, peptide hormones, and associated GPCRs are potential targets for novel insecticides since they take place in metabolic, reproductive, developmental, and behavioral pathways in insects [165,166]. Neurohormone and neuropeptide GPCRs are expressed as well as their ligands in insects. For example, allatostatin receptors, tachykinin receptors, adipokinetic and Corazon hormone receptors, and more have been

annotated [134]. There is only one commercial pesticide called Amitraz that functions via the Octopamine receptor, which is a class A GPCR [167]. It works against a wide variety of insects [168, 169]. However, it has toxic effects on animals and humans, causing respiratory failure, unconsciousness, and hemodynamic instability [170, 171].

Figure 1.3 represents how GPCRs are targeted as novel pesticide candidates. While computer-based approaches accelerate finding the appropriate molecule for the target GPCR, candidate compounds are evaluated *in vitro* to ensure their efficacy. Molecules with detectable action are tested in the target organism, and pesticide activity is evaluated.

1.10. Insects

Regarding the number of species and individuals, insects are the most varied animal taxon. There are around one million insect species described, with the true number likely to be five to ten times higher. In contrast, the total number of individual insects is believed to reach one million trillion [172, 173].

There is evidence that the relative age of insects has increased their species diversity, providing time for evolution and low extinction rates [174]. Flight can increase variety in terms of morphological, ecological, or behavioral assumptions, such as greater dispersion, wing folding, metamorphosis, and ecological niche [175].

1.10.1. Pine Processionary Moth

Thaumetopoea pityocampa (Denis and Schiffermüller)(T.pit) from the Lepidoptera: Notodontidae family, also known as the pine processionary moth, is a species primarily found in the Mediterranean region [176]. These pests, which mainly harm pine trees, feed on pine needles and cause serious damage to these plants. In addition, they pose a serious health threat to humans, and pets [177]. Due to global warming, pine processionary moth is expanding towards Northern regions where they can survive better since they are temperature-sensitive species [178].

T. pit's biological cycle includes both an aerial and a terrestrial cycle. The aerial phase commences with the formation of the moth and the development of the egg into larvae. Female moths can lay 70-300 eggs at the crowns of pine trees only once. Larva formation takes about 5-6 weeks. They stay together as larvae attached to pine needles and weave a net as a nest. They migrate in a one-line pattern at night, following remnants of pheromones. In the aerial stage, T. pit goes through 5 instar stages. They can only withstand temperatures ranging from 20 to 25 degrees. The aerial period lasts from March until June. Caterpillars look for a warm, well-lit location to spend a month in the terrestrial phase and transform into a chrysalis. The adult moth is nocturnal. Based on climatic conditions, the biological cycle of T. pit can span over the years (2–5) [179].

T.pit larvae feed on pine needles and cause severe damage to pine trees. If they are present in large numbers, they cause death by completely defoliating young and old trees. They also damage trees, making them vulnerable to attack by fungi and other wood-boring insects. This situation generates ecological damage as well as economic losses. Moreover, health issues arising from T. pit concern humans and animals [180,181]. Urticarial hairs of caterpillars become airborne with a peak in April and May and penetrate the skin. Contact with air dispersed urticarial hairs cause skin rash and urticaria as well as ocular and respiratory afflictions, which are extremely dangerous for asthma patients [182].

These insects, which are now spreading to more places with global warming, cause severe concerns and need to be controlled [183]. Existing methods to combat the pine scavenger defense are to destroy egg batches and silk nests physically or chemically. In addition, pheromone traps, essential oils, microbial pathogens, and natural predators *Calosoma sycophanta* are used [184]. However, all of these methods are effective to a limited extent, creating the need for a more effective pesticide. For this reason, the pine processionary moth is a good pesticide target [185, 186].

2. PURPOSE

Insect GPCRs are potential novel pesticide targets since they take place in metabolic, reproductive, developmental, and behavioral pathways in insects. Pine processionary moth larvae feed on pine needles and cause severe damage to pine forests. This situation generates ecological and economic damages. Contact with urticarial hairs of larvae causes health problems in humans and animals.

The purpose of this study was to identify the allosteric binding pockets of the AstR-C by utilizing in silico and in vitro methods of allosteric ligand discovery. In addition, we aimed to obtain molecules that work more effectively by decreasing the EC50 values and showing cooperation with the agonists we found for the AstR-C receptor. We believed this study would contribute to designing a more specific and selective pesticide, thus a safer pesticide for *Thaumetopoea pityocampa*.

3. MATERIALS

3.1. Reagents, Kits, and Enzymes

Reagents, kits, and enzymes used in this study are listed in Table 3.1.

Table 3.1. List of reagents, kits, and enzymes.

Name	Supplier
Dulbecco's Modified Eagle Medium (DMEM)	PAN-Biotech, Germany
Fetal Bovine Serum (FBS)	Gibco, UK
Penicillin-Streptomycin (10X)	Pan-Biotech, Germany
Lipofectamine 3000 Transfection Reagent	Thermo Fisher Scientific, USA
Promega cAMP-Glo™ Assay Kit	Promega, USA
TrypLE™ Express Enzyme (1X), phenol red	Gibco, UK
Opti-MEM™ Reduced Serum Medium, no phenol red	Gibco, UK

3.2. Biological Materials

3.2.1. Mammalian Cell Lines

For cell culture procedures, human embryonic kidney cell line HEK293 was used.

3.3. Nucleic Acids

3.3.1. List of Plasmids

pcDNA3.1(+) (Invitrogen, CA, USA) plasmids containing AP-TGFα, ASTR-C, Gα protein were used in this study.

3.4. Chemicals, Buffers, and Solutions

Chemicals, buffers, and solutions used in this study are listed in Table 3.2.

Table 3.2. Chemicals, Buffers, and Solutions.

Name	**Supplier**
Bovine Serum Albumin (BSA)	AppliChem, Germany
Ethanol	Tekkim, Turkey
Calcium Chloride	Sigma, UK
D-Glucose	Sigma, UK
DMSO	Sigma, UK
Hank's Balanced Salt Solution (HBSS)	
HEPES	Bioshop Canada Inc.
Magnesium Chloride ($MgCl_2$)	Sigma, UK
Magnesium Chloride Hexahydrate ($MgCl_2.6H_2O$)	Merck, Germany
Magnesium Sulfate Heptahydrate ($MgSO_4{\cdot}7H_2O$)	Merck, Germany
p-Nitrophenyl Phosphate (p-NPP)	Merck, Germany
Phosphate Buffered Saline (PBS)	MP Biomedicals, France
,Potassium Chloride (KCl)	Sigma, UK
Potassium Phosphate Monobasic (KH_2PO_4)	Merck, Germany
Sodium bicarbonate ($NaHCO_3$)	Merck, Germany
Sodium chloride (NaCl)	Sigma, UK
Sodium Phosphate Dibasic Dihydrate ($Na_2HPO_4{\cdot}2H_2O$)	Merck, Germany
Tris-HCl	Thermo Fisher Scientific, USA

3.4.1. Culture Media

Cell culture media was prepared by supplementing 10% Fetal Bovine Serum (FBS), 1% Penicillin/Streptomycin, and 1% Glutamine.

3.5. List of Disposable Labware

Disposable labware that is used in this study is listed in Table 3.3.

Table 3.3. List of disposable labware.

Name	Supplier
Cell Culture Plates (6-well, 96-well)	TPP, Switzerland
Cell Culture Flasks (T25, T75)	TPP, Switzerland
Centrifuge Tubes (15 ml)	Capp, Denmark
Centrifuge Tubes (50 ml)	Corning, USA
Cryovial Tubes	
Microfuge Tubes (1.5 ml, 2 ml)	Axygen, USA
Pipette Tips (Filtered)	Capp, Denmark
Pipette Tips (Bulk)	VWR, USA
Serological Pipettes (5 ml, 10 ml, 25 ml)	Capp, Denmark

3.6. Peptide

AST-C peptide of *Thaumetopoea pityocampa* was ordered COMPANY NAME.

3.7. Molecules

Two small molecules from FDA approved drug library were ordered from Vitas-M Laboratories. Other small molecules from Life Chemicals GPCR 2D Similarity Focused Library Allosteric Subset and SPECS library were ordered from MolPort.

3.8. List of Equipments

Pieces of equipment used in this study are listed in Table 3.4.

Table 3.4. List of equipment.

Name	**Supplier**
Autoclave	Midas 55, Prior Clave, UK
Carbon dioxide tank	Genç Karbon, Turkey
Cell culture incubator	Hepa Class 100, Thermo, USA
Centrifuge	Allegra X-30, Beckman Coulter, USA
Cold room	Birikim Elektrik Soğutma, Turkey
Deep freezers	-20 °C, Bosch, Germany -80 °C ULT Freezer, Thermo Fisher Scientific, USA -150 °C, MDF-1156, Sanyo, Japan
DRI-Block DB-2A	Techne, UK
Hemocytometer	Weber Scientific International Ltd, UK
Ice Machine	Scotsman Inc., AF20, Italy
Laboratory Bottles	Isolab, Germany
Laminar Flow Cabinet	Labcaire BH18, UK
Magnetic Stirrers	M221 Elektromag, Turkey
Micropipettes	Eppendorf, Germany
CKX41 Inverted Microscope	Olympus Life Sciences, Japan
Motorized Pipette Controller	Capp, Denmark
Fluoroskan Ascent FL	Thermo Fisher Scientific, USA
Vortexmixer VM20	Chiltern Scientific, UK

3.9. Online Tools and Software

Allosite 2.0 and Protein Allosteric Regulatory Sites (PARS) online tools were used in this study. The software that were used is listed in Table 3.5.

Table 3.5. List of online tools and software.

Name	**Supplier**
AutoDock Vina	AutoDock Suite
Excel	Microsoft Office 365
Desmond	Schrödinger, Inc. New York, 2018, USA
Glide	Schrödinger, Inc. New York, 2018, USA
GraphPad Prism 9.3.1	California, USA
LigPrep	Schrödinger, Inc. New York, 2018, USA
Maestro	Schrödinger, Inc. New York, 2018, USA
MarvinSketch 20.21.0	ChemAxon Ltd., Budapest, Hungary
MDpocket	Fpocket 2.0
OPM Database	University of Michigan
Prime	Schrödinger, Inc. New York, 2018, USA
Protein Preparation Wizard	Schrödinger, Inc. New York, 2018, USA
Pymol	Schrödinger, Inc. New York, 2018, USA
PyRx Virtual Screening Tool 8.0	PyRx
SiteMap	Schrödinger, Inc. New York, 2018, USA
VMD	University of Illinois, 1995-2013

4. METHODS

4.1. Computational Studies

4.1.1. Protein Preparation

Computational procedures on protein require protein preparation step to check the structure properties and fix if any problems are present. The Protein Preparation Wizard module implemented in the Maestro (Schrödinger Release 2018-4: Maestro, Schrödinger, LLC, New York, NY, 2021.) was used for this purpose. Protein refinement and minimization steps were applied while protonation states were at pH 7.0. OPLS3e force field [187] were used for minimization and optimization.

4.1.2. Text-Mining in Ligand Libraries

FDA Approved Drugs and SPECS libraries were imported to MarvinSketch 20.21.0, (C) 2000-2020 ChemAxon Ltd., and ligands were converted to IUPAC name format. Coumarin derivatives related to the receptor were sorted through text mining and converted back to ligand structures. These ligands were used to build sub-libraries only containing coumarin derivatives of FDA and SPECS libraries.

4.1.3. Ligand Library Preparation

Life Chemicals GPCR 2D Similarity Focused Library Allosteric Subset was downloaded from Life Chemicals. Ligand libraries must be prepared before the docking applications. LigPrep module (LigPrep Schrödinger Release 2018-4: LigPrep, Schrödinger, LLC, New York, NY, 2021.) was used. OPLS3e force field was utilized, and PROPKA was used for protonation states at pH 7.0 +/- 2.0.

4.1.4. Allosteric Pocket Prediction

4.1.4.1. Allosite 2.0. Allosite 2.0 is an allosteric pocket prediction server supported by a Support Vector Machine (SVM) algorithm [188]. The active state structure of AstR-C, which was previously built with homology modeling by our group, was submitted to the server.

4.1.4.2. Protein Allosteric Regulatory Sites (PARS) . PARS server uses flexibility and structural conversation of proteins to detect allosteric sites [189]. Apo structure of the protein was uploaded to the server. For the settings, predict protein binding sites, check conservation, and active site residues options were chosen. Analysis of the results was conducted according to the guideline provided by the server.

4.1.4.3. Sitemap. Sitemap (Schrödinger Release 2018-4: SiteMap, Schrödinger, LLC, New York, NY, 2021.) is a module that investigates protein surfaces to detect possible binding sites. An evaluation was led according to pocket size, solvent exposure, and hydrophobic character, which was followed by the scoring of the sitemaps. The prepared structure of the receptor was imported to Sitemap, and settings were calibrated to a minimum of 15 site points per reported site and a maximum number of 7 sites to report at the end of the analysis. For hydrophobicity, more restrictive definitions were set, and sitemaps were trimmed at 4 Å from the nearest site point.

4.1.4.4. MDpocket. MDpocket is a binding pocket detection program that uses a geometry-based site detection algorithm [190]. The trajectory of 200 ns molecular dynamics (MD) simulation of the receptor was subjected to analysis. Results were visualized and analyzed in VMD software [191].

4.1.4.5. Blind-Docking. Blind-docking is a useful method if there is no prior knowledge of binding sites. This method uses the entire receptor surface to detect binding pockets. Glide (Schrödinger Release 2018-4: Glide, Schrödinger, LLC, New York, NY, 2021.)

and AutoDock Vina [192] programs were used to apply blind-docking on the protein with the prepared ligand libraries.

Before blind-docking with Glide, a grid was generated by the Receptor Grid Generation module. Grid box center coordinates were (0, 0, 0) and inner box (40, 40, 40) and outer box (50, 50, 50) sizes were calibrated to cover the receptor surface. The Standard Precision (SP) method was used with flexible ligand sampling. Epik state penalties were added, and rewarding the intramolecular hydrogen bonds were included besides enhancing the planarity of the conjugated pi groups. Five poses were included per ligand, and post-docking minimizations were applied.

PyRx 8.0 [193] accommodating AutoDock Vina was used for blind-docking. The grid box size and center were calibrated to encapsulate the whole receptor, and the exhaustiveness level was set to 8.

4.1.5. Virtual Screening

Virtual screening was applied to allosteric site candidates using the previously prepared ligand libraries.

4.1.5.1. Glide. The grids of the allosteric sites were generated with the Receptor Grid Generation module based on the coordinates of the produced sitemaps. Previously described blind-docking settings were used for virtual screening with Glide.

4.1.5.2. AutoDock Vina. The same procedure was applied to AutoDock Vina for virtual screening after adjusting the docking coordinates to allosteric sites.

4.1.6. Simulation System Building

The orientation of the ligand-bound receptor structures was obtained after submitting the structures to the Orientation of Proteins in Membranes (OPM) database

[194]. Desmond System Builder (Schrödinger Release 2018-4: Desmond Molecular Dynamics System, D. E. Shaw Research, New York, NY, 2021. Maestro-Desmond Interoperability Tools, Schrödinger, New York, NY, 2021.) module of Maestro was used to build the biological system for MD simulations. The receptor was embedded in a POPC (1-palmitoyl-2-oleoyl-sn-glycerol-3-phosphocholine) lipid bilayer. The simulation system consisted of TIP3P clear water, counterions, and 0.15 M NaCl.

4.1.7. Molecular Dynamics Simulations

Desmond Molecular Dynamics System (Schrödinger Release 2022-2: Desmond Molecular Dynamics System, D. E. Shaw Research, New York, NY, 2021. Maestro-Desmond Interoperability Tools, Schrödinger, New York, NY, 2021.) was utilized for MD simulations, and OPLS3e force field was used. The equilibrium step was performed with the default algorithm. The temperature was 310 K, and the pressure was 1.01325 bar. The Nose−Hoover thermostat and the Martyna−Tobias−Klein barostat methods were applied to the system. The calculation of the long-range electrostatic interactions was achieved by the particle mesh Ewald method. A cut-off radius of 9.0 Å was used for both van der Waals and Coulombic interactions, and the time-step was assigned as 2.0 fs. An NPγT ensemble was used with a surface tension of 4000 bar/Å. 100 ns and 200 ns MD simulations were performed with three independent replica simulations.

4.1.8. Analysis of MD Simulations

Analysis of the simulations was performed by Simulation Interactions Diagram (SID) module. The trajectories that were collected during simulations were used for the examination. An analysis report was produced by the program.

4.1.9. Root Mean Square Deviation

RMSD is used to assess the accuracy of protein-ligand docking algorithms and conformation sampling techniques [195, 196]. RMSD is typically calculated using only heavy atoms [197].

RMSD Equation: RMSD is calculated as follows

$$\mathrm{RMSD} = \sqrt{\frac{1}{N}\sum_{i=1}^{N}\delta_i^2} \tag{4.1}$$

where δi is the distance between atom i and either a reference structure or the mean position of the N equivalent atoms.

4.1.10. Root Mean Square Fluctuation

The root mean-square-average distance between an atom and its average position in a particular set of structures is defined as RMSF for a specific number of structures [198–200]. **RMSF Equation:** RMSF is calculated as follows

$$\mathrm{RMSF} = \sqrt{\frac{1}{N}\sum_{j}^{N}\left(x_i(j) - (x_i)\right)^2}. \tag{4.2}$$

4.1.11. Molecular Mechanics/Generalized Born Surface Area Analysis

The average of non-strain ΔG (ΔG-NS) is calculated by the script. Dividing ΔG-NS by the number of the heavy atoms of each ligand, the binding efficiency was calculated. ΔG-NS will be denoted as "ΔG" in the rest of the text.

4.2. Mammalian Cell Culture Studies

4.2.1. Growth and Maintenance of HEK293 Cells

HEK293 cells were seeded and grown on 75 cm^2 cell culture flasks. Cells were maintained in Dulbecco's modified eagle medium (DMEM) (PAN-Biotech, Germany) supplied with 10% FBS (Gibco, UK), 1% Penicillin/Streptomycin (Hyclone, USA), and 1% L-Glutamine (Gibco, UK). Complete DMEM was restored at 4 °C, and it was incubated at 37 °C Dri-Block before usage. Cells were incubated at 37 °C incubator and supplied with 5% CO_2.

4.2.2. Cell Passage

Cells were subcultured when they were at 70-80% confluency. The old medium was aspirated, and cells were washed with 1X PBS. After aspirating the PBS, cells were treated with 2-3 volume TrypLE Express Enzyme for 2 minutes at 37 °C. Equal amounts of complete DMEM were added, and cells were resuspended and transferred to a falcon tube. Subsequently, cells were centrifuged at 500 x g for 3 minutes, and the supernatant was discarded. Cells were resuspended in fresh complete media and seeded on a 1:4 ratio.

4.2.3. Cryopreservation

Cells were frozen at 80-90% confluency to prepare frozen cell stocks. After aspirating the old medium and washing with PBS, cells were detached and centrifuged at 500 x g for 5 minutes. Eventually, the supernatant was removed, and cells were resuspended in freshly prepared 4 °C freezing media containing DMEM supplied with 10% DMSO and 10% FBS. 1 ml of cell suspension containing 1-2 million cells were transferred into every 2 ml screw-capped cryotubes.

4.2.4. Thawing

Complete media supplied with 15% FBS were prewarmed to 37 °C. Cells were rapidly warmed to 37 °C and transferred into a 15 ml falcon tube containing 9 ml prewarmed media and centrifuged at 500 x g for 5 minutes. The supernatant was aspirated, and cells were resuspended in fresh complete media and seeded on 25 cm^2 flask.

4.2.5. Transient Transfection

Transfected cells were used in shedding and cAMP accumulation assays. Cells were seeded in a 6-well plate at 70-80% confluency one day before the transfection. Lipofectamine 3000 Transfection Reagent was used for transfection according to the

manufacturer's instructions. Cells were transfected with AstR-C, Gαi subtypes, and AP-TGFα plasmids.

4.2.6. Peptide and Small Molecule Dissolvation

The AST-C peptide was dissolved in PBS supplemented with 0.1% BSA. The final concentration was 1 mM. Small molecules were dissolved in DMSO.

4.2.7. TGF-α Shedding Assay

The method was applied according to the original protocol [201]. Cells were transfected one day ago from the shedding assay. The transfected cells were washed with PBS and detached with TrypLE. After stopping the enzyme's activity with the addition of DMEM, the cell suspension was centrifuged at 190 x g for 5 minutes. The supernatant was aspirated, and cell pellets were resuspended in 3 ml PBS and incubated for 5 minutes at room temperature. Cells were centrifuged again at the same settings, and the supernatant was removed by aspiration. The cell pellet was resuspended in 4 ml HBSS containing 5 mM HEPES (pH 7.4). The cell suspension was transferred into a 96-well plate, 100 μl per well, and incubated for 30 minutes in a cell culture incubator.

After 30 minutes of incubation, re-seeded cells were treated with 10 μl 10X ligand concentrations as schematized in the Table 4.1. The plate was mixed by gentle tapping and placed into an incubator for 1 hour. After incubation with the ligands, the plate was centrifuged at 190 x g for 2 minutes. 80 μl per well-conditioned media were transferred into an empty 96-well plate. the p-NPP-containing solution must be prepared fresh on the day from the stock. p-NPP solution prewarmed to 37 °C were added 80 μl per well to both conditioned media and cell plates. Plates were incubated at 37 °C for 5 minutes. Plates were analyzed in a microplate reader and measured the absorbance at 405 nm. Measurements were repeated at 1 hour and 2 hours later. Data processing was accomplished as suggested by the authors.

Table 4.1. Ligand concentrations.

COMPOUNDS	**CONCENTRATION**
AST-C EC20	0.09 nM
AST-C EC80	13 nM
Allosteric Ligand 1X	0.01 nM
	0.1 nM
	1 nM
	10 nM
	100 nM
	1 μM
	10 μM
	100 μM

5. RESULTS

5.1. Allosteric Pocket Prediction

The allosteric pocket detection process was accomplished by comparing the outcome of different software and servers. All pocket predictions were numbered to establish a more uniform and understandable results section since each algorithm produces many results with different names and numerations.

5.1.1. MDpocket

MDpocket analysis was executed with a 200 ns MD simulation of the apo form AstR-C and produced fifteen pockets in total (Figure 5.1). The first pocket (Pocket1) was found on the lower half of transmembrane (TM) domains 1 and 2. Pocket2 was detected in the upper part of TM 2-3, while Pocket3 was located in the upper half of TM 3-4. Pocket4 is a cavity formed by TM 2-3-4 domains detected near the Na^+ binding site prominently found in Class A GPCRs and known for allosteric modulation. The cavity was elongated towards the center of the receptor and predominantly formed by the $D^{2.50}$ and $S^{2.39}$ residues which support the Na^+ binding site location. D(E)RY is another micro switch that is important for the allosteric network of GPCRs, and Pocket5 was detected next to $D^{3.49}$-$R^{3.50}$-$Y^{3.51}$ residues and site resided between TM 3-4 and ICL-2. In the middle axis between the TM 3-4-5 domains, Pocket6 was found. Pocket7 was identified in the cavity formed by TM 4-5, and it was located closer to the ECL-2. It should be noted that, especially for the opioid-like GPCRs, ECL-2 is a key part of the GPCR activation mechanism. A very small cavity, Pocket9, was found at the tail of the TM 5 in the intracellular part of the receptor. Above the highly conserved $W^{6.48}$ residue and near the Q271 residue identified as vital for AstR-C receptor activity, Pocket10 was detected. Pocket11 was detected below the Pocket10 and resided at the central axis of the protein, and it was smaller compared to the previous one. Two pockets were identified between TM 6-7, and Pocket12 was located closer to the extracellular part. On the other hand, Pocket13 was located at

the intracellular part, next to the C-terminus domain. Upwards to $N^{7.45}$ Pocket15 was identified. Binding sites indicating the orthosteric and g-protein binding sites were numbered as Pocket18 and Pocket19, respectively.

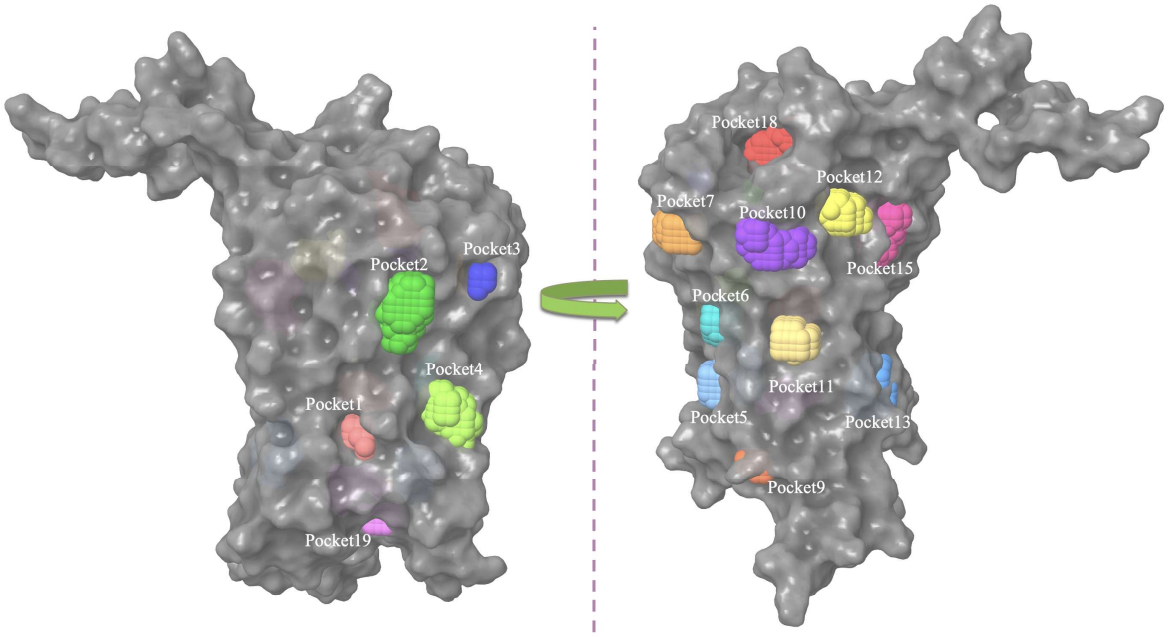

Figure 5.1. MDpocket predictions.

5.1.2. Allosite

Allosite analysis yielded three binding sites, Pocket10, Pocket18, and Pocket19, as shown in Figure 5.2. Analysis's outputs were given as pocket volume, total solvent accessible surface area (SASA), feature score (logitProb), perturbation score (nmaScore), and allosite score (hitScore). Topological and physiological features of the allosteric site were used for a logistic regression model to calculate the logitProb score ranging from 0 to 1. nmaScore was obtained from normal mode analysis, and it points out the allosteric effect. hitScore was obtained from the combination of logitProbe and nmaScore.

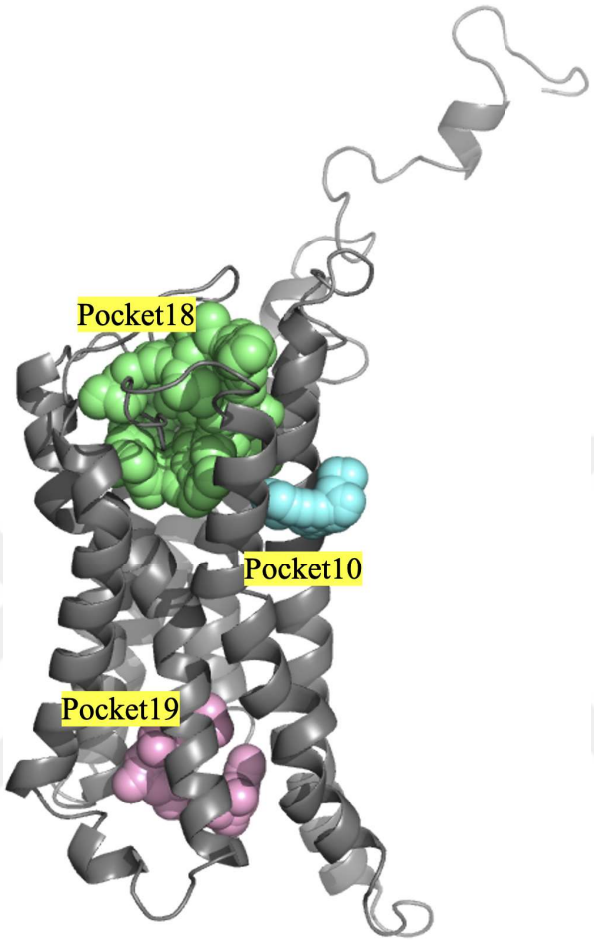

Figure 5.2. Allosite pocket predictions.

Table 5.1. Allosite pocket prediction results.

Feature	**Pocket10**	**Pocket18**	**Pocket19**
Volume	370.925	2002.383	818.895
SASA	168.097	373.183	168.097
Druggability Score	0.692	0.171	0.692
logitProb	0.458	0.410	0.458
nmaScore	1.000	1.000	1.000
hitScore	0.567	0.528	0.567

5.1.3. PARS

PARS server inquires about allosteric regulatory sites through evaluating protein flexibility and structural conservation. PARS analysis resulted in four conserved and four flexible cavities (Figure 5.3). Structural conservation scores above the 50% were considered significant and colored in cyan. The highest structural conservation score (StrCon) was obtained by Pocket5, which was located between TM 3-4 and ICL-2, near the highly conserved D134$^{3.49}$ of the DRY motif. Pocket17 was spotted in the center of the receptor, deeply buried in the central axis. Pocket18 was detected in the orthosteric site, whereas Pocket 19 was located in the G-protein binding site.

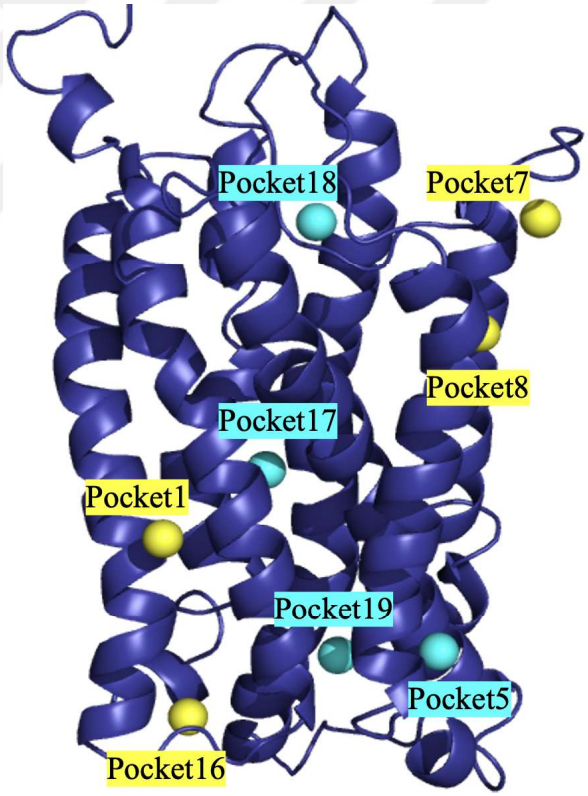

Figure 5.3. PARS predictions.

Yellow-colored cavities were indicators of flexibility, labeled where the p-value was lower than 0.05. Flexibility scores (pFlex scores) show that binding a ligand to these labeled yellow cavities can alter the overall protein conformation, and scores were listed in Table 5.2. Pocket1 was located between TM 1 and 2, near the conserved D$^{2.50}$.

Pocket7 was detected between TM 4-5 and ECL-2, whereas Pocket8 resided below that region. Finally, Pocket16 was observed around the C-terminal, between TM 1-7.

Table 5.2. PARS analysis results.

Site	**pFlex**	**StrCon**
Pocket1	0.76	0
Pocket5	0.70	100.0
Pocket7	0.74	0
Pocket8	0.63	20.0
Pocket16	0.71	0
Pocket17	0.83	60.0
Pocket18	0.55	80.0
Pocket19	0.46	60.0

5.1.4. Sitemap

SiteMap analysis resulted in five potential binding sites. Site1 (Pocket18) indicated the entrance of the orthosteric site, while Site2 (Pocket19) showed the entrance of the G-protein binding site. Site3 (Pocket7) is positioned in the cavity formed by TM domains 4 and 5 and ECL-2 encompassing residues W191, P192, K194, D195, L196, N197, K198, G199, T202, F203, and Y206. Site5 (Pocket8) is below Site3, next to TM domains 4 and 5, consisting of F122, V168, P171, I172, F203, Y206, S207, and L210. Site4 (Pocket5) is in the intracellular region of the receptor, a cavity formed by the TM domains 3 and 4 and ICL-2, covering residues Y76, I130, A133, D134, I137, A145, L148, R149, V153, I156, V157. Sitemap analysis results were presented in Table 5.3 and binding sites were demonstrated in Figure 5.4.

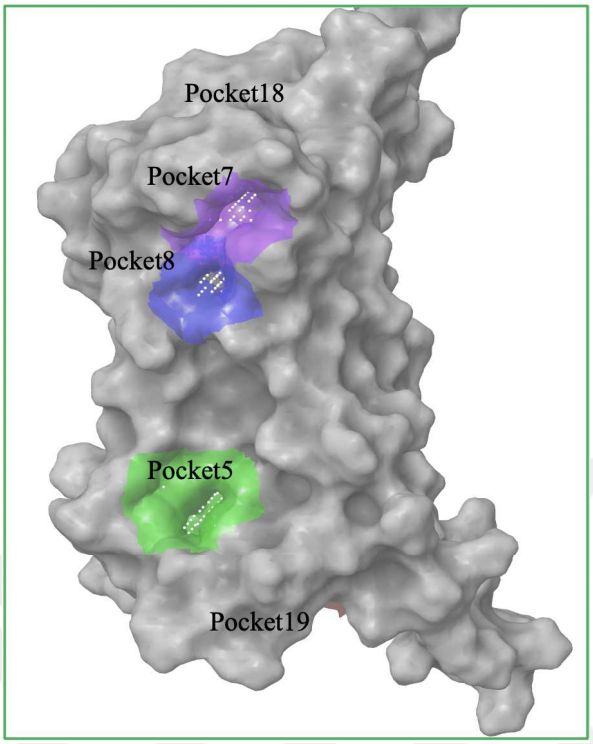

Figure 5.4. Sitemap analysis results.

Table 5.3. Sitemap analysis results.

	Pocket5	**Pocket7**	**Pocket8**	**Pocket18**	**Pocket19**
SiteScore	758	648	728	1.132	867
Size	32	30	21	227	49
Dscore	762	569	743	1.156	867
Volume	67.228	71.001	44.933	657.531	215.747
Exposure	595	559	596	395	712
Enclosure	659	668	660	860	732
Contact	842	951	928	1.126	837
Phobic	1.886	117	2.123	1.170	916
Philic	508	1.065	258	920	705
Balance	3.714	110	8.225	1.272	1.299
Donor/Acceptor	1.713	425	2.201	757	1.102

5.1.5. Blind-Docking

Blind-docking was accomplished by two software. Blind docking using Glide revealed three different possible binding sites. The first ligand population was found in the previously described orthosteric pocket (Pocket18). The second binding site (Pocket7) was located between the transmembrane domains 4 and 5 and ECL-2, comprising the residues V168, P171, W191, P192, K194, D195, K198, G199, F203, and S207. The third indicated a cavity formed by I82, C86, I119, N120, W162, A166, M169, T170, and F173 residues dispersed around TM domains 2, 3, and 4 (Pocket4).

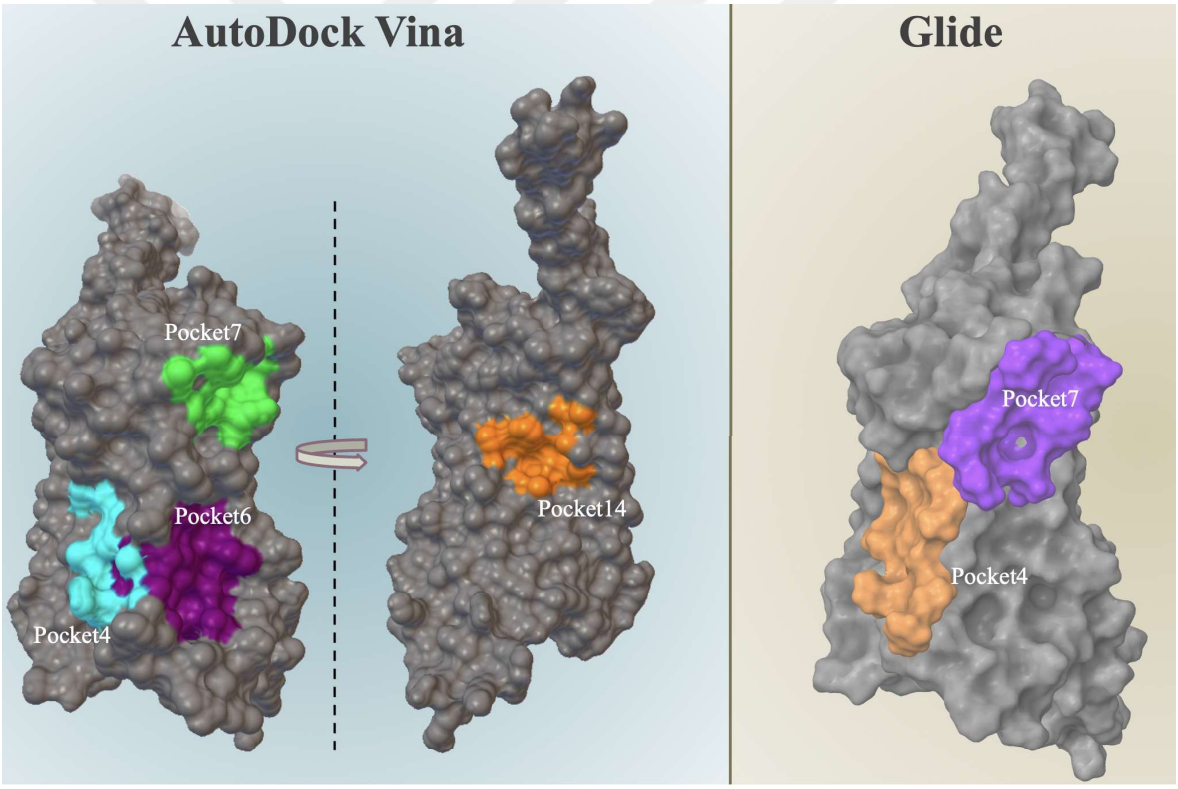

Figure 5.5. Blind-docking results of Glide and AutoDock Vina.

Blind-docking with AutoDock Vina resulted in five binding sites. Compounds were dispersed to the firstly orthosteric site. Secondly, a cavity formed by I82, A83, E85, C86, S116, T117, I119, N120, A161, W162, T163, S165, A166, and M169 residues on the TM domains 2, 3, 4 (Pocket4), and a region near the TM domains 3, 4, and 5 (Pocket6) with residues F127, L128, I130, A133, D134, L148, S154, V157, and A160.

The fourth site was detected between TM 4, 5, and ECL2 (Pocket7) with residues V168, M169, P171, W191, P192, D195, L196, G199, Q200, T202, F203, and Y206, and lastly, a site formed by A41, L44, V48, C263, W264, P266, F297, Y299, N301, and S302 was detected on TM 6, 7, and 1 (Pocket14). The detected pockets by Glide and AutoDock Vina were presented in Figure 5.5.

Allosteric sites were chosen by comparing the reproducing regions in the results of different analysis techniques. The predicted allosteric pocket was compared and examined, and it was seen that there were three major binding sites. These are the sites positioned in TM 3-4 and ICL-2 (Pocket5), TM 4-5 and ECL-2 (Pocket7), and TM 4-5 (Pocket8).

5.2. Virtual Screening to Find Allosteric Modulators

5.2.1. Sitemap Docking

The allosteric pocket prediction was followed by searching allosteric ligands that bind to allosteric sites. For this purpose, three ligand libraries were employed, which were GPCR 2D Similarity Focused Library Allosteric Subset of Life Chemicals (LC) and chromen-2-one derivatives from FDA and SPECS libraries. The virtual screening approach was applied to previously decided sites Pocket5, Pocket7, and Pocket8 with these libraries separately using Glide software's Standard Precision (SP) method.

The highest score was observed in Pocket7 with F0214-0057. However, the average docking scores of each library were better in Pocket5. LC library produced the best scores. Interestingly, the top compound from the FDA coumarin derivatives was the same in Pocket5 and Pocket8, which was the Hymecromone molecule.

For Pocket7, the highest docking scores were obtained from the LC library. SPECS coumarin derivatives showed higher affinity towards Pocket7 compared to FDA coumarin molecules. In the case of Pocket8, results similar to Pocket7 were observed, although higher docking scores were produced on this site compared to the previous

one. Docking scores of the highest ranked molecules from each library were listed in Table 5.4.

Table 5.4. Virtual screening results.

Library	**Pocket5**	**Gscore**	**Pocket7**	**Gscore**	**Pocket8**	**Gscore**
LC	F0266-2714	-6.782	F2147-1744	-6.457	F0214-0057	-7.020
FDA	Hymecromone	-6.118	Iliparcil	-5.766	Hymecromone	-5.629
SPECS	AQ-150/42303585	-6.252	A0-022/43453354	-5.656	AE-848/31922060	-6.460

5.3. Molecular Dynamics Simulations with Allosteric Modulator Candidates

Molecular dynamics (MD) simulations are useful tools to measure protein-ligand complex stability and to observe the interactions between them. Firstly, hit molecules were subjected to 100 ns MD simulations with AstR-C based on their docking pose, and these compounds were presented in Figure 5.6.

Nine 100 ns long MD simulations were applied to three molecules for each binding site. Some of these compounds could not sustain their interaction with the protein until the end of the simulations. In Pocket5, F0266-2714/protein interaction was lost, although other molecules kept their association with the receptor. A similar situation was observed in Pocket7 with the Iliparcil molecule, which had lost its connection to the protein. However, all molecules in the Pocket8 sustained the interplay throughout the 100 ns simulations. The molecules that maintained their exchange with the receptor were subjected to 200 ns long MD simulations for further examination.

Simulations were conducted with the remaining seven molecules with the same settings but with a longer duration. Hymecromone and AQ-150/42303585 maintained their interaction in the Pocket5 for 200 ns. In Pocket7, F2147-1744 and A0-022/43453354 preserved their connection to the binding site. Whereas, in Pocket8, AE-848/31922060 lost contact towards the end of the simulation. However, the other two molecules, F0214-0057 and Hymecromone, remained in the pocket until the end of the simulations.

Chemical Formula	Compound Name
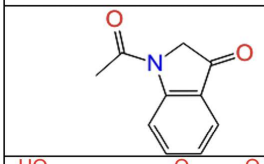	F0266-2714
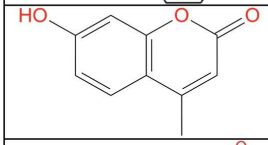	Hymecromone
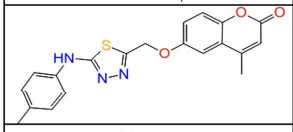	AQ-150/42303585
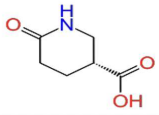	F2147-1744
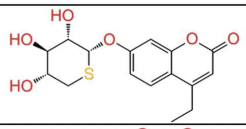	Iliparcil
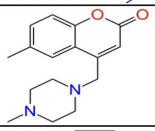	A0-022/43453354
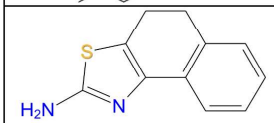	F0214-0057
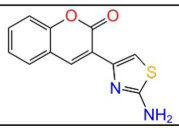	AE-848/31922060

Figure 5.6. Top 3 molecules for each binding site were subjected to MD simulations.

Further analysis of the simulation trajectories gives more information about the interplay between ligands and the protein. H-bond between Asp134 residue and OH-group of the Hymecromone in Pocket5 was significantly persistent, and it was present 99 % of the 200 ns simulation (Figure 5.7A). Asp134 was a part of the D(E)RY motif in GPCR A family, which is essential for G-protein coupling. Observing a strong H-bond interaction during the simulation may be an indicator of the molecule's modulator role. Tyr76, also near the DRY motif, was another residue that Hymecromone frequently interacted with 39 % of the time, and H-bonds and hydrophobic interactions were detected. Hydrophobic interactions built by Ile137 and Val157 were also detected.

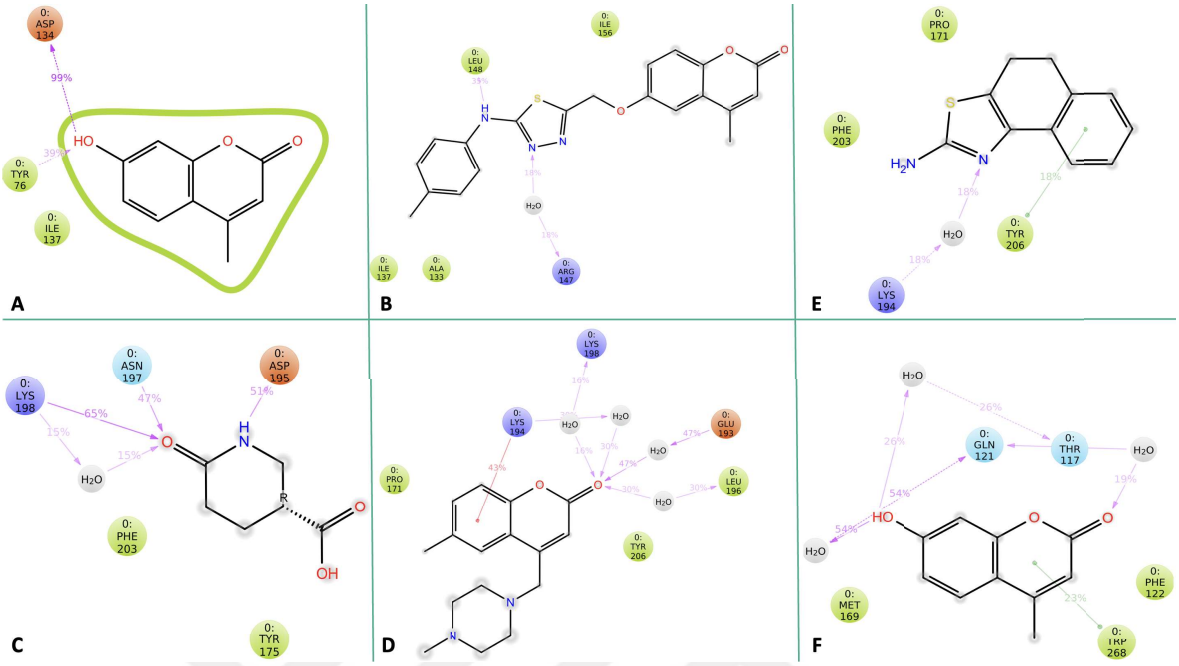

Figure 5.7. Ligand contacts information from the MD simulations.

AQ-150/42303585 was the second molecule that bound to Pocket5. The simulation analysis showed that many hydrophobic interactions were present alongside the water bridges and H-bonds (Figure 5.7B). Leu148 was the most interacted residue with H-bond to the amino group of the AQ-150/42303585. There was a hydrogen bond between the Arg147 residue and the thiadiazol group of the ligand-mediated by a water molecule. The hydrophobic interactions with the Ile156 were the most frequent alongside other residues. It should be noted that there were some associations with the DRY motif residues throughout the simulation.

The next analyzed trajectory was AstR-C/F2147-1744. Pocket7 was detected near the ECL-2, and in this complex, F2147-1744 mostly interacted with ECL-2 residues such as Tyr175 and Gly199 (Figure 5.7C). Hydrogen bonds and water bridges were prominent in the binding site, especially with Lys198. H-bonds between Asp195 with the piperidine ring and Asn197 with the oxygen atom of the piperidine ring were detected in 50 % of the simulation. Some hydrophobic connections were also present with TM-5 residues such as Thr202, Phe203, Tyr206, and Ser207.

A0-022/43453354's interaction with the receptor was focused on ECL-2 residues. Protein-ligand interplay mainly comprised water bridges and hydrophobic interactions (Figure 5.7D). The key residue was Lys194 since it interacted with Pocket7 for the duration. Lys194 exchanged π-cation bonds and water bridges with the coumarin ring. Glu193, Leu196, and Lys198 were the other ECL-2 residues contributing to the protein-ligand interplay. Tyr206 residue was also a great contributor to interactions with the hydrophobic interactions that it provided.

The AstR-C/F0214-0057 simulation showed that the ligand interacted with ECL-2 and the transmembrane residues. However, compared to Pocket7, transmembrane residues were more prominent in the interaction, which was expected since Pocket8 is located below the Pocket7. Tyr206 residue was associated with the ligand's dihydro naphthalene group through π-π stacking (Figure 5.7E). Lys194 and thiazol group of the ligand interacted with water bridges. Pro171, Phe203, and Leu210 exchanged hydrophobic bonds with the molecule, whereas Tyr175, Val190, Lys194, and Gln200 cooperated through water bridges.

Lastly, Hymecromone in Pocket8 was investigated. Analysis of collected trajectories produced various interactions. For instance, a water bridge between Gln121 and the ligand's hydroxy group was present 80 % of the time (Figure 5.7F). Hydrophobic interactions with the Phe122 and π-π stacking between Trp268 and coumarin ring were significant, which is important to note that this residue is located above the highly conserved $W^{6.48}$ which is critical for GPCR activation.

In Figure 5.8 RMSD values that were gathered from the analysis of 200 ns MD simulation trajectories were represented. Protein Cα RMSD values can inform the conformational changes within the protein and its stability. As seen in all graphs, the protein Cα RMSD values were not fixed at the beginning of the simulations but reached equilibrium and remained at around 2-3 Å until the end. On the other hand, receptor/Hymecromone in the Pocket5 complex reached the equilibrium later compared to other systems.

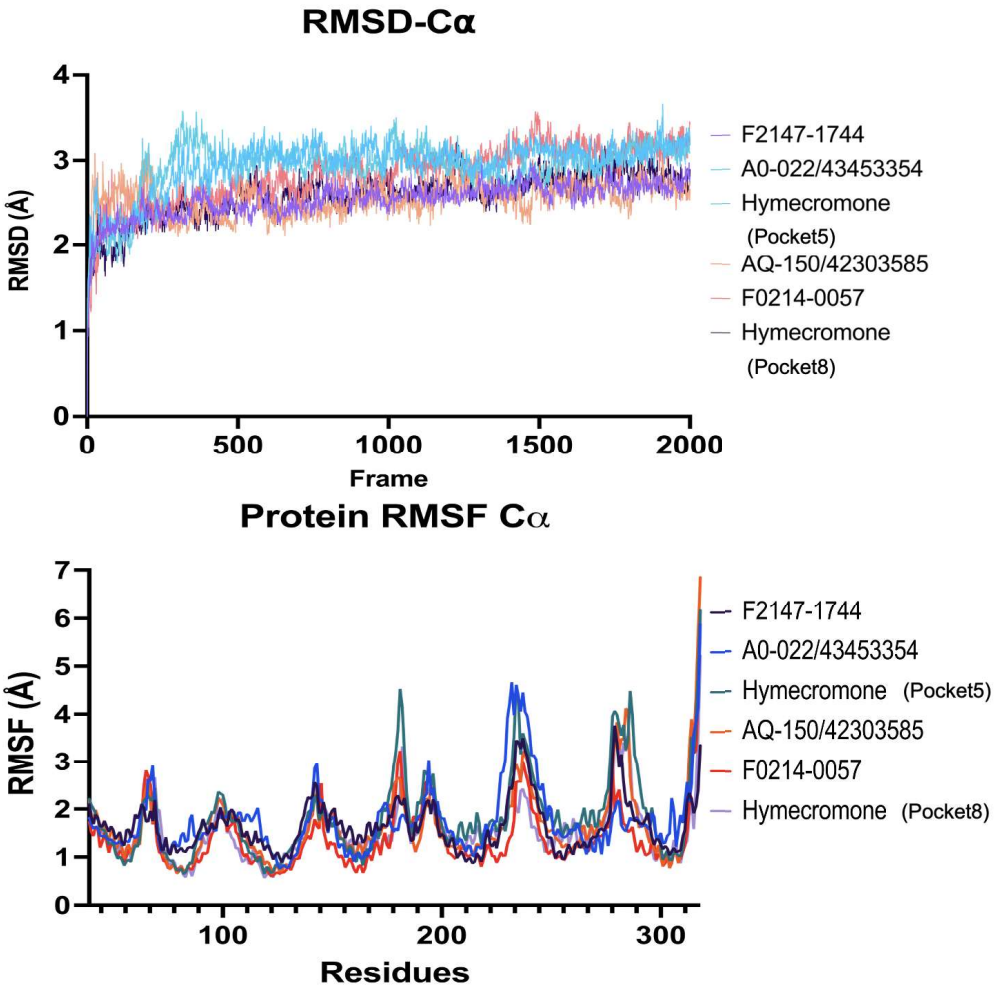

Figure 5.8. Comparison of 200 ns MD simulations Cα RMSD and RMSF values of AstR-C with ligands.

In Figure 5.9, Protein Cα, ligand fit on protein, and ligand fit on ligand RMSD values were represented for each simulation. Ligand fit protein RMSD was calculated through aligning ligand heavy atoms on the protein-ligand complex, which was aligned on the reference protein backbone. The ligand fit ligand was measured by aligning the ligand on its initial conformation.

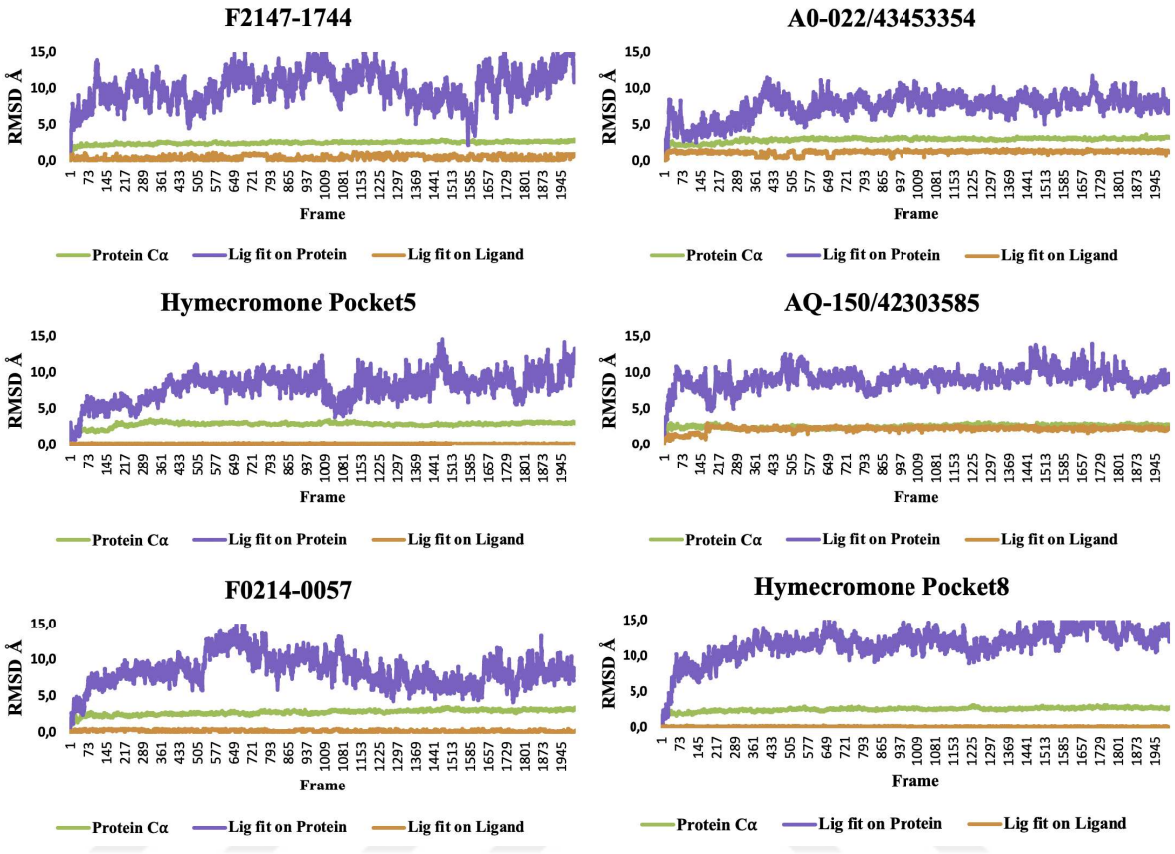

Figure 5.9. RMSD graphs of ligands bound to AstR-C for 200 ns.

5.4. Free Energy Calculations

100 frames from the MD simulation trajectories were chosen for binding free energy (ΔG) calculations. The Molecular Mechanics with Generalised Born and Surface Area Solvation (MM/GBSA) method was used to estimate ΔG values of the protein-ligand complexes. ΔG values in Figure 5.10 were calculated without considering the energy required to perform the conformational changes to form the protein-ligand complex, and NS means "no strain" energy. AQ-150/42303585 had the highest binding energy with an average of -45.043 ±5.534 kcal/mol. F0214-0057 had the second highest ΔG score with an average score of -41.801 ±4.904 kcal/mol. MM-GBSA analysis results of the other molecules were: F2147-1744 with an -37.662 ±5.583 kcal/mol, Hymecromone in Pocket5 -37,441 ±2.941 kcal/mol, A0-022/43453354 -32.237 ±4.422 and lastly Hymecromone in Pocket8 -30.537 ±2.602.

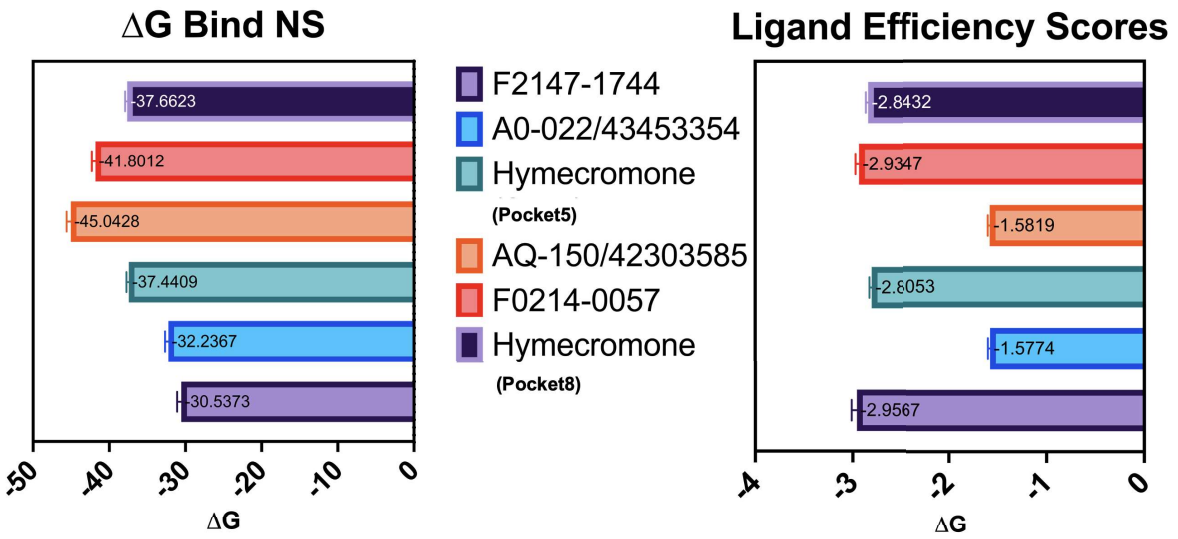

Figure 5.10. Binding free energy and ligand efficiency scores of 200 ns MD simulations of AstR-C with ligands.

Ligand efficiency score means binding free energy per ligand atom except for the hydrogen atoms. The highest ligand efficiency score was obtained by F2147-1744 with an -2.957 ±0.548 kcal/mol. Free energy values per atom for the other ligands were: A0-022/43453354 -1.577 ±0.219 kcal/mol, Hymecromone in Pocket5 -2.805 ±0.224 kcal/mol, AQ-150/42303585 -1.582 ±0.196 kcal/mol, F0214-0057 -2.935 ±0.353, and Hymecromone in Pocket8 -2.843 ±0.212 kcal/mol.

5.5. Cell Signaling Assays

Allosteric molecules were tested using shedding assays EC20 and EC80 concentrations of the AST-C peptide and results were presented in Figure 5.11. Among the molecules, it is seen the Hymecromone molecule stands out clearly. It significantly increased the AT-TGF-α response by increasing the activity of AST-C at EC20 concentration. The EC50 value of Hymecromone was determined to be 41.328 μM. It showed the same positive modulator effect at the EC80 AST-C concentration, but the max response remained the same. This may be due to the saturation effect of Hymecromone.

AQ-150/42303585 molecule slightly increased AST-C efficacy, yet the max response was the same with only AST-C peptide. F0214-0057 could not be tested via shedding assay. A0-022/43453354 showed a mixed response; it decreased the activity of AST-C at EC20 concentration, although it increased the shedding at EC80 concentration. Any cooperativity between F2147-1744 and AST-C peptide was not observed.

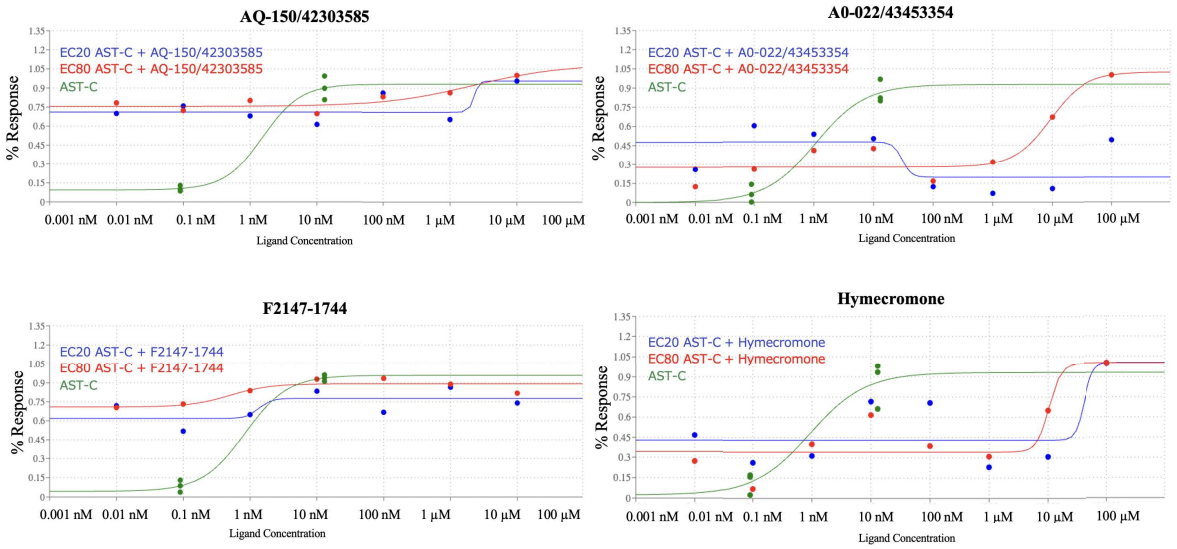

Figure 5.11. TGF-α Shedding Assay results of allosteric molecules with AST-C peptide.

6. DISCUSSION AND CONCLUSION

GPCRs are multifunctional receptors that have roles in many physiological pathways. They are the largest group of cell receptors and are expressed ubiquitously in humans, and other species [165]. For instance, neuropeptide receptors are responsible for regulating various vital pathways such as reproduction, metamorphosis, and development [166]. Since they are fundamental for insect metabolism, they represent potential pesticide targets. Currently used conventional pesticides have been carrying out many questions regarding their safety issues. Environmental contamination, bioaccumulation, toxicity, and pest resistance are just examples of the current concerns in pesticide usage [129]. However, pesticides have been a part of human life for decades and provided many benefits, such as enhancing crop yield and quality, preventing diseases, and providing affordable food, which also helps advanced nutrition. Since pesticides have many benefits undeniably, it is essential to assess the drawbacks and target these problems. Increasing selectivity and target-specificity while avoiding causing non-target effects and other toxic side effects must be considered throughout the pesticide design process, which may help maintain balance in pesticide usage. Accordingly, it leads to increasing demand for safer next-generation pesticides, and GPCRs are good candidates since they regulate many physiological signaling cascades in insects.

GPCRs are popular drug targets, covering a large part of the drugs on the market. Many drugs that target GPCRs are designed for orthosteric pockets. Orthosteric sites are easy to find and located on the extracellular side, which makes them easy to reach by the drugs since they do not have to pass through the cell membrane. However, it may cause side effects since orthosteric pocket residues are highly conserved among the GPCRs, and it decreases the selectivity of the drugs and results in unwanted effects [101]. Nevertheless, orthosteric pockets are not the only available sites. Allosteric sites are dispersed around the receptor structure and can mediate receptor signaling remotely. Allosteric pockets provide new opportunities to target GPCRs. Ligands targeting allosteric areas can mediate orthosteric ligand activity, increase receptor

specificity, reduce side effects and risk of overdose, and enhance ligand efficiency [62]. Although it is challenging to target allosteric pockets, it has the potential to provide solutions for the current apprehensions.

Allatostatin C is a neuropeptide that inhibits Juvenile hormone synthesis, which is the mediator of reproduction, sex pheromones, metamorphosis, growth, and development in insects [202]. Allatostatin type C receptor is a class A GPCR, and when activated by its respective allatostatin ligand, the receptor inhibits the Juvenile hormone synthesis in the Corpora Allata. Because of its mandatory role in insect metabolism, Allatostatin receptors are prospective pesticide targets [203].

In a previous study of our group, the AstR-C receptor of Pine Processionary Moth was characterized, and its 3D structure was built with homology modeling [185]. Its orthosteric pocket and natural ligand (AST-C) were identified. Drug screening was applied to discover small molecules that can activate AstR-C. In this study, we identified allosteric binding sites of AstR-C of T. pit through various *in silico* methods such as blind-docking and pocket prediction algorithms based on normal mode analysis and perturbation analysis, and applied virtual screening to allosteric pockets for allosteric modulator discovery.

The first step was to identify the allosteric binding sites of the AstR-C. For this purpose, different allosteric pocket detection algorithms were utilized. Allosite server is a platform built for allosteric pocket detection, which uses the Support Vector Machine algorithm trained in the allosteric database (ASD). Analysis of AstR-C by Allosite server resulted in three binding sites located at orthosteric (Pocket18) and G-protein binding sites (Pocket19) and between TM 5-6 domains (Pocket10). PARS server was the second online tool to investigate allosteric sites. It inquiries allosteric sites by evaluating the flexibility and structural conservation and scores them.

PARS analysis resulted in eight binding sites; half of them were flexible cavities, and half were structurally conserved sites among the GPCR A family. Orthosteric and G-protein binding sites were among the conserved cavities. Pocket17 was deeply

buried in the receptor center, a common orthosteric site for GPCRs. The last conserved cavity was Pocket5, located between the TM 3-4 and ICL-2 domains and next to the DRY motif. Pocket5 also had a high flexibility score, which was necessary for allosteric pockets since they modulate receptor activity through conformational changes. It was also remarkable that this site was detected around a highly conserved motif and microdomain, which is a part of the shared allosteric network of the GPCR activation mechanism. Pocket1 was marked as a flexible cavity and detected between TM 1-2, near the conserved $D^{2.50}$ of Na^+ pocket. The collapse of the Na^+ pocket and repacking $D^{2.50}$ residue with several TM 7 and TM 3 residues mediates the movement of TM 7 to TM 3 allosterically, which leads to receptor activation. The high flexibility and connection to the allosteric network of Pocket1 were noticeable, although it had a meager structural conservation score. Pocket7 and Pocket8 were identified between TM 4-5 and the ECL-2 region and labeled as flexible. ECL-2 is known for mediating orthosteric and allosteric ligand binding class A GPCRs, and there are several crystal structures resolved with an allosteric ligand such as M2 muscarinic acetylcholine receptor and GPR40 [204, 205]. Loop regions show high mobility and sequence variety, contributing to receptor selectivity and different activation modes. Pocket16 was observed around the C-terminal, between TM 1-7. Since C-terminal has roles in G-protein activation and inward/outward movement of TM 7 is important for forming the G-protein binding site, Pocket16 may be associated with Gα recruitment to the receptor.

Sitemap analysis led to five binding sites, two of which were orthosteric and G-protein binding sites, and the rest were previously mentioned Pocket5, Pocket7, and Pocket8. Pocket7 had a more hydrophilic character than the other two, which was expected since it was positioned towards the extracellular site near the ECL-2 domain. Pocket8 was more hydrophobic than Pocket5, and the reason must be that the binding site was facing the lipid bilayer of the cell membrane, whereas Pocket5 was residing towards the intracellular part. Detection of the same three binding sites with a different software could indicate their modulating role and predisposition to be a binding pocket.

Apo form of AstR-C was subjected to 200 ns MD simulation, and the collected trajectory was submitted to MDpocket analysis. MDpocket analysis was advantageous

since it did not accomplish the evaluation of only one structure but a 200 ns trajectory which contained 2000 frames of the receptor. Thus, it was able to detect fifteen cavities throughout differing protein conformations. The cavities were identified all around the receptor; some were more prominent based on their location and pocket size. Pocket4 was detected in this analysis, too, but differently, the cavity was elongated to the receptor center through a small entrance. MDpocket also identified Pocket5 near the DRY motif and Pocket7 near the ECL-2. Pocket10, previously determined by Allosite, was also observed near the Q271 residue, which was stated as crucial for AstR-C in a previous work of our group. A new cavity was found around $N^{7.49}$ residue, which makes contact with the Na^{+} pocket during the receptor activation alongside the $N^{7.45}$ and $S^{3.39}$.

Blind-docking is helpful for scanning the entire protein surface to identify possible binding cavities. For this approach, two software were used with three ligand libraries. Standard Precision docking with Glide resulted in three binding sites. The vast majority of the ligands were bound to the orthosteric site. However, noticeably two ligand population was observed in Pocket4 and Pocket7 too. When blind-docking was applied with ADT Vina, five pockets were discriminated. Similarly, most of the ligands were bound to the orthosteric site, and Pocket4 and Pocket7 were perceived by ADT Vina too. Additionally, Pocket6 and Pocket14 were identified.

Crystal structures of previously defined allosteric binding sites, data on allosteric sites of GPCR A class in the literature, and repetitive results in different analyzes were considered during allosteric pocket determination. Furthermore, pocket size and depth, position on the receptor, and its score were contemplated. As a result, three cavities were distinguished: Pocket5, Pocket7, and Pocket8. These sites were observed in the outcomes of different applications repetitively. TM 3-4 and ICL-2 region and TM 4-5 and ECL-2 region are hotspots for GPCR A family allostery. Pocket5 region was reported for Adenosine A2A receptor, β2-AR, GPR40, C5a [204, 206–208]. For the ECL-2 region, the M2 receptor has two crystal structures solved with agonist and PAMs [41]. It was also noticeable that these binding sites were positioned where mobility is high, which helps to perform conformational changes. ECL-2 domain has

roles in ligand selectivity as well as receptor activation. In the case of AstR-C, the orthosteric pocket is not localized deep in the receptor but around the extracellular loops, especially ECL-2. The position and the length of ECL-2 enable building contacts with several transmembrane α helices such as TM 4, TM 5, TM 3, and TM 6. Thus, Pocket7 and Pocket8 may be associated with mediating orthosteric ligand binding. In the case of Pocket5, its position is directly linked to the allosteric network of the receptor through the DRY microdomain and hydrophobic arginine cage. Accordingly, this site might be related to conformational changes occurring in ligand stimulation.

Following the allosteric pocket determination, virtual screening was applied to binding sites with three ligand libraries to discover allosteric modulators. The same ligand libraries were used in docking to the orthosteric pocket to compare the docking scores. Hit molecules of allosteric pockets had higher scores in allosteric sites than in the orthosteric pocket. The highest score was -7.020 gscore obtained by F0214-0057 in Pocket8. Hymecromone molecule was the top scored compound for Pocket5 and Pocket8 from the FDA library, which may be related to the hydrophobic nature of these regions. Top molecules from each library were chosen for further procedures, and three compounds for each site, nine molecules in total, were used in MD simulations.

Ligand-bound receptor structures were submitted to 100 ns MD simulations at the beginning, and subsequently, the complexes that sustained their interactions were presented to 200 ns simulations. Trajectories were analyzed through RMSD and RMSF values and protein-ligand contacts. Since the N-terminal of the receptor is very long and mobile, it fluctuates excessively and increases RMSD and RMSF values. Thus, it was not included in RMSD and RMSF graphs. Loop domains are other particularly mobile regions, and fluctuations can be noticed in the RMSF plot. Examination of the trajectories showed that interactions in Pocket5 were mostly hydrophobic interactions and polar interactions involving DRY motif residues. Whereas protein-ligand contacts were maintained through polar interactions and water bridges supplied by primarily ECL-2 residues in Pocket7. Likewise, water bridges were observed alongside the hydrophobic interactions like π-π stacking in Pocket8, more transmembrane residues were present in these interactions. Comparison of the protein Cα RMSD values showed that

F2147-1744 bound in Pocket7 complex was more stable.

After evaluating the simulations, two molecules for each site were used in free energy calculations. MM-GBSA analysis was performed using 100 frames from each trajectory. AQ-150/42303585 had the highest ΔG score with an average of -45.043 $\pm$5.534 kcal/mol. However, the highest ligand efficiency score was obtained by F2147-1744 with an -2.957 $\pm$0.548 kcal/mol.

Five molecules were tested *in vitro* with TGF-α shedding assay. When only allosteric molecule candidates were used for the stimulation, agonist or antagonist activities were not observed. Allosteric molecules were also tested with AST-C to detect cooperativity. Hymecromone molecule was the only significant positive modulator that was detected. Although minor changes were observed in the shedding results of AST-C with EC20 and EC80 concentrations, no significant effect was observed for other molecules.

Identified binding sites must be verified further with *in vitro* studies. For this purpose, binding pockets can be targeted using site-directed mutagenesis, and the effects of deformations on the receptor can be examined. These effects may take a role in the receptor stability or its ligand binding capacity. In parallel with *in vitro* methods, mutations in binding pockets can be subjected to molecular dynamics simulations and observed what kind of conformational changes they cause. It should be considered when evaluating the results that while determining the allosteric binding sites, the 3D model is used instead of the crystal structure of the AstR-C receptor of *T.pit.* Although three ligand libraries were used, simulations were continued with a relatively small number of molecules. This number could be increased, or molecule screening could be continued with other libraries. Allosteric molecules were tested with TGF-α shedding assay alone and with the EC20 and EC80 concentrations of AST-C peptide. Since no allosteric agonist or antagonist effects were observed, they can be expected to work cooperatively with another molecule. However, since the impact of allosteric molecules is probe dependent, they should be tested with as many ligands as possible, and their effects should be examined. In addition, it should be verified whether allosteric modulator

candidates bind to the determined allosteric pockets with cell-based assays. For this purpose, binding can be verified using FRET or BRET, which are based on examining interactions of fluorescent-labeled ligands and pockets. The effect of the allosteric candidates and their cooperative ligands must be tested in bioassays on the physiology of pine processionary moth.

This study determined allosteric binding pockets and allosteric modulator candidates that can contribute to designing a next-generation pesticide targeting the pine processionary moth. Developing safer and more effective drugs against pests is essential, and new steps are taken in this direction every day; it is believed that this study will contribute to such studies.

REFERENCES

1. Filmore, D., "It's A GPCR World", *Modern Drug Discovery*, Vol. 7, pp. 24–28, 2004.

2. Venkatakrishnan, A., T. Flock, D. E. Prado, M. E. Oates, J. Gough and M. M. Babu, "Structured and Disordered Facets of the GPCR Fold", *Current Opinion in Structural Biology*, Vol. 27, pp. 129–137, 2014.

3. Lee, S.-M., J. M. Booe and A. A. Pioszak, "Structural Insights Into Ligand Recognition and Selectivity for Classes A, B, and C GPCRs", *European Journal of Pharmacology*, Vol. 763, pp. 196–205, 2015.

4. Congreve, M., C. de Graaf, N. A. Swain and C. G. Tate, "Impact of GPCR Structures on Drug Discovery", *Cell*, Vol. 181, pp. 81–91, 2020.

5. Cong, X., J. Topin and J. Golebiowski, "Class A GPCRs: Structure, Function, Modeling and Structure-Based Ligand Design", *Current Pharmaceutical Design*, Vol. 23, pp. 4390–4409, 2017.

6. Bermudez, M. and A. Bock, "Does Divergent Binding Pocket Closure Drive Ligand Bias for Class A GPCRs?", *Trends in Pharmacological Sciences*, Vol. 40, pp. 236–239, 2019.

7. Hollenstein, K., C. de Graaf, A. Bortolato, M.-W. Wang, F. H. Marshall and R. C. Stevens, "Insights Into the Structure of Class B GPCRs", *Trends in Pharmacological Sciences*, Vol. 35, pp. 12–22, 2014.

8. Chun, L., W.-h. Zhang and J.-f. Liu, "Structure and Ligand Recognition of Class C GPCRs", *Acta Pharmacologica Sinica*, Vol. 33, pp. 312–323, 2012.

9. Dor, A., K. Okrasa, J. Patel, M. Serrano-Vega, K. Bennett, R. Cooke, J. Errey,

A. Jazayeri, S. Khan and B. Tehan, "Structure of Class C GPCR Metabotropic Glutamate Receptor 5 Transmembrane Domain", *Nature*, Vol. 551, pp. 557–562, 2014.

10. Velazhahan, V., N. Ma, G. Pándy-Szekeres, A. J. Kooistra, Y. Lee, D. E. Gloriam, N. Vaidehi and C. G. Tate, "Structure of the Class D GPCR Ste2 Dimer Coupled to Two G Proteins", *Nature*, Vol. 589, pp. 148–153, 2021.

11. Hu, G.-M., T.-L. Mai and C.-M. Chen, "Visualizing the GPCR Network: Classification and Evolution", *Scientific Reports*, Vol. 7, pp. 1–15, 2017.

12. Schulte, G. and P. Kozielewicz, "Structural Insight Into Class F Receptors-What Have We Learnt Regarding Agonist-Induced Activation?", *Basic and Clinical Pharmacology and Toxicology*, Vol. 126, pp. 17–24, 2020.

13. Wright, S. C., P. Kozielewicz, M. Kowalski-Jahn, J. Petersen, C.-F. Bowin, G. Slodkowicz, M. Marti-Solano, D. Rodríguez, B. Hot and N. Okashah, "A Conserved Molecular Switch in Class F Receptors Regulates Receptor Activation and Pathway Selection", *Nature Communications*, Vol. 10, pp. 1–12, 2019.

14. Kozielewicz, P., A. Turku and G. Schulte, "Molecular Pharmacology of Class F Receptor Activation", *Molecular Pharmacology*, Vol. 97, pp. 62–71, 2020.

15. Alkhalfioui, F., T. Magnin and R. Wagner, "From Purified GPCRs to Drug Discovery: The Promise of Protein-Based Methodologies", *Current Opinion in Pharmacology*, Vol. 9, No. 5, pp. 629–635, 2009.

16. Sanchez-Reyes, O. B., A. L. Cooke, D. B. Tranter, D. Rashid, M. Eilers, P. J. Reeves and S. O. Smith, "G Protein-Coupled Receptors Contain Two Conserved Packing Clusters", *Biophysical Journal*, Vol. 112, pp. 2315–2326, 2017.

17. Cvicek, V., W. A. Goddard and R. Abrol, "Structure-Based Sequence Alignment of the Transmembrane Domains of All Human GPCRs: Phylogenetic, Structural

and Functional Implications", *PLOS Computational Biology*, Vol. 12, p. e1004805, 2016.

18. Haneef, S. A. S. and S. Ranganathan, "Structural Bioinformatics Analysis of Variants on GPCR Function", *Current Opinion in Structural Biology*, Vol. 55, pp. 161–177, 2019.

19. Jacob, C. and N. W. Bunnett, "Transmembrane Signaling by G Protein-Coupled Receptors", *Physiology of the Gastrointestinal Tract*, pp. 63–90, Elsevier Academic Press, 2006.

20. Oldham, W. M. and H. E. Hamm, "Heterotrimeric G Protein Activation by G-Protein-Coupled Receptors", *Nature Reviews Molecular Cell Biology*, Vol. 9, pp. 60–71, 2008.

21. Wingert, B., P. Doruker and I. Bahar, "Activation and Speciation Mechanisms in Class A GPCRs", *Journal of Molecular Biology*, p. 167690, 2022.

22. Tehan, B. G., A. Bortolato, F. E. Blaney, M. P. Weir and J. S. Mason, "Unifying Family A GPCR Theories of Activation", *Pharmacology and Therapeutics*, Vol. 143, pp. 51–60, 2014.

23. Ballesteros, J. A. and H. Weinstein, "Integrated Methods for the Construction of Three-Dimensional Models and Computational Probing of Structure-Function Relations in G Protein-Coupled Receptors", *Methods in Neurosciences*, Vol. 25, pp. 366–428, Elsevier, 1995.

24. Xie, X.-Q. and A. Chowdhury, "Advances in Methods to Characterize Ligand-Induced Ionic Lock and Rotamer Toggle Molecular Switch in G Protein-Coupled Receptors", *Methods in Enzymology*, Vol. 520, pp. 153–174, Elsevier, 2013.

25. Zhou, X. E., K. Melcher and H. E. Xu, "Structure and Activation of Rhodopsin", *Acta Pharmacologica Sinica*, Vol. 33, pp. 291–299, 2012.

26. Schneider, E. H., D. Schnell, A. Strasser, S. Dove and R. Seifert, "Impact of the DRY Motif and the Missing "Ionic Lock" on Constitutive Activity and G-Protein Coupling of the Human Histamine H4 Receptor", *Journal of Pharmacology and Experimental Therapeutics*, Vol. 333, pp. 382–392, 2010.

27. Bakker, R. A., A. Jongejan, K. Sansuk, U. Hacksell, H. Timmerman, M. R. Brann, D. M. Weiner, L. Pardo and R. Leurs, "Constitutively Active Mutants of the Histamine H1 Receptor Suggest A Conserved Hydrophobic Asparagine-cage That Constrains the Activation of Class AG Protein-Coupled Receptors", *Molecular Pharmacology*, Vol. 73, pp. 94–103, 2008.

28. Olivella, M., G. Caltabiano and A. Cordomí, "The Role of Cysteine 6.47 in Class A GPCRs", *BMC Structural Biology*, Vol. 13, pp. 1–11, 2013.

29. Latorraca, N. R., A. Venkatakrishnan and R. O. Dror, "GPCR Dynamics: Structures in Motion", *Chemical Reviews*, Vol. 117, pp. 139–155, 2017.

30. Preininger, A. M., J. Meiler and H. E. Hamm, "Conformational Flexibility and Structural Dynamics in GPCR-mediated G Protein Activation: A Perspective", *Journal of Molecular Biology*, Vol. 425, pp. 2288–2298, 2013.

31. Jaakola, V.-P., M. T. Griffith, M. A. Hanson, V. Cherezov, E. Y. Chien, J. R. Lane, A. P. Ijzerman and R. C. Stevens, "The 2.6 Angstrom Crystal Structure of A Human A2A Adenosine Receptor Bound to An Antagonist", *Science*, Vol. 322, pp. 1211–1217, 2008.

32. Doré, A. S., N. Robertson, J. C. Errey, I. Ng, K. Hollenstein, B. Tehan, E. Hurrell, K. Bennett, M. Congreve, F. Magnani *et al.*, "Structure of the Adenosine A2A Receptor in Complex With ZM241385 and the Xanthines Xac and Caffeine", *Structure*, Vol. 19, pp. 1283–1293, 2011.

33. Massink, A., H. Gutiérrez-de Terán, E. B. Lenselink, N. V. O. Zacarías, L. Xia, L. H. Heitman, V. Katritch, R. C. Stevens and A. P. IJzerman, "Sodium Ion

Binding Pocket Mutations and Adenosine A2A Receptor Function", *Molecular Pharmacology*, Vol. 87, pp. 305–313, 2015.

34. Gutiérrez-de Terán, H., A. Massink, D. Rodríguez, W. Liu, G. W. Han, J. S. Joseph, I. Katritch, L. H. Heitman, L. Xia, A. P. IJzerman *et al.*, "The Role of A Sodium Ion Binding Site in the Allosteric Modulation of the A2A Adenosine G Protein-Coupled Receptor", *Structure*, Vol. 21, pp. 2175–2185, 2013.

35. Trzaskowski, B., D. Latek, S. Yuan, U. Ghoshdastider, A. Debinski and S. Filipek, "Action of Molecular Switches in GPCRs-Theoretical and Experimental Studies", *Current Medicinal Chemistry*, Vol. 19, pp. 1090–1109, 2012.

36. Bissaro, M., G. Bolcato, G. Deganutti, M. Sturlese and S. Moro, "Revisiting the Allosteric Regulation of Sodium Cation on the Binding of Adenosine at the Human A2A Adenosine Receptor: Insights From Supervised Molecular Dynamics (SuMD) Simulations", *Molecules*, Vol. 24, p. 2752, 2019.

37. Tautermann, C. S., D. Seeliger and J. M. Kriegl, "What Can We Learn From Molecular Dynamics Simulations for GPCR Drug Design?", *Computational and Structural Biotechnology Journal*, Vol. 13, pp. 111–121, 2015.

38. Gurevich, V. V. and E. V. Gurevich, "Molecular Mechanisms of GPCR Signaling: A Structural Perspective", *International Journal of Molecular Sciences*, Vol. 18, 2017.

39. Zhou, Q., D. Yang, M. Wu, Y. Guo, W. Guo, L. Zhong, X. Cai, A. Dai, W. Jang, E. I. Shakhnovich, Z.-J. Liu, R. C. Stevens, N. A. Lambert, M. M. Babu, M.-W. Wang and S. Zhao, "Common Activation Mechanism of Class A GPCRs", *eLife*, Vol. 8, p. e50279, 2019.

40. Huang, W., A. Manglik, A. J. Venkatakrishnan, T. Laeremans, E. N. Feinberg, A. L. Sanborn, H. E. Kato, K. E. Livingston, T. S. Thorsen, R. C. Kling, S. Granier, P. Gmeiner, S. M. Husbands, J. R. Traynor, W. I. Weis, J. Steyaert,

R. O. Dror and B. K. Kobilka, "Structural Insights Into μ-Opioid Receptor Activation", *Nature*, Vol. 524, No. 7565, pp. 315–321, 2015.

41. Kruse, A. C., A. M. Ring, A. Manglik, J. Hu, K. Hu, K. Eitel, H. Hübner, E. Pardon, C. Valant, P. M. Sexton, A. Christopoulos, C. C. Felder, P. Gmeiner, J. Steyaert, W. I. Weis, K. C. Garcia, J. Wess and B. K. Kobilka, "Activation and Allosteric Modulation of A Muscarinic Acetylcholine Receptor", *Nature*, Vol. 504, pp. 101–106, 2013.

42. Lohse, M. J., I. Maiellaro and D. Calebiro, "Kinetics and Mechanism of G Protein-Coupled Receptor Activation", *Current Opinion in Cell Biology*, Vol. 27, pp. 87–93, 2014.

43. Manglik, A. and A. C. Kruse, "Structural Basis for G Protein-Coupled Receptor Activation", *Biochemistry*, Vol. 56, pp. 5628–5634, 2017.

44. Adjobo-Hermans, M. J., J. Goedhart, L. van Weeren, S. Nijmeijer, E. M. Manders, S. Offermanns and T. W. Gadella, "Real-Time Visualization of Heterotrimeric G Protein Gq Activation in Living Cells", *BMC Biology*, Vol. 9, p. 32, 2011.

45. Moreira, I. S., "Structural Features of the G-Protein/GPCR Interactions", *BBA-General Subjects*, Vol. 1840, pp. 16–33, 2014.

46. Zhou, X. E., K. Melcher and H. E. Xu, "Structural Biology of G Protein-Coupled Receptor Signaling Complexes", *Protein Science*, Vol. 28, pp. 487–501, 2019.

47. Schmidt, C., T. Thomas, M. Levine and E. Neer, "Specificity of G Protein Beta and Gamma Subunit Interactions.", *Journal of Biological Chemistry*, Vol. 267, pp. 13807–13810, 1992.

48. Mahoney, J. P. and R. K. Sunahara, "Mechanistic Insights Into GPCR-G Protein Interactions", *Current Opinion in Structural Biology*, Vol. 41, pp. 247–254, 2016.

49. Smith, J. S. and S. Rajagopal, "The β-Arrestins: Multifunctional Regulators of

G Protein-Coupled Receptors", *Journal of Biological Chemistry*, Vol. 291, pp. 8969–8977, 2016.

50. Latorraca, N. R., J. K. Wang, B. Bauer, R. J. L. Townshend, S. A. Hollingsworth, J. E. Olivieri, H. E. Xu, M. E. Sommer and R. O. Dror, "Molecular Mechanism of GPCR-Mediated Arrestin Activation", *Nature*, Vol. 557, pp. 452–456, 2018.

51. Shenoy, S. K. and R. J. Lefkowitz, "Multifaceted Roles of β-Arrestins in the Regulation of Seven-Membrane-Spanning Receptor Trafficking and Signalling", *Biochemical Journal*, Vol. 375, pp. 503–515, 2003.

52. Asher, W. B., D. S. Terry, G. G. A. Gregorio, A. W. Kahsai, A. Borgia, B. Xie, A. Modak, Y. Zhu, W. Jang, A. Govindaraju, L. Y. Huang, A. Inoue, N. A. Lambert, V. V. Gurevich, L. Shi, R. J. Lefkowitz, S. C. Blanchard and J. A. Javitch, "GPCR-Mediated β-Arrestin Activation Deconvoluted With Single-Molecule Precision", *Cell*, Vol. 185, pp. 1661–1675.e16, 2022.

53. Gurevich, V. V. and E. V. Gurevich, "GPCR Signaling Regulation: The Role of GRKs and Arrestins", *Frontiers in Pharmacology*, Vol. 10, p. 125, 2019.

54. Pack, T. F., M. I. Orlen, C. Ray, S. M. Peterson and M. G. Caron, "The Dopamine D2 Receptor Can Directly Recruit and Activate GRK2 Without G Protein Activation", *Journal of Biological Chemistry*, Vol. 293, pp. 6161–6171, 2018.

55. Latorraca, N. R., M. Masureel, S. A. Hollingsworth, F. M. Heydenreich, C.-M. Suomivuori, C. Brinton, R. J. Townshend, M. Bouvier, B. K. Kobilka and R. O. Dror, "How GPCR Phosphorylation Patterns Orchestrate Arrestin-Mediated Signaling", *Cell*, Vol. 183, pp. 1813–1825.e18, 2020.

56. Weis, W. I. and B. K. Kobilka, "The Molecular Basis of G Protein-Coupled Receptor Activation", *Annual Review of Biochemistry*, Vol. 87, pp. 897–919, 2018.

57. Springael, J. Y., C. de Poorter, X. Deupi, J. V. Durme, L. Pardo and M. Parmen-

tier, "The Activation Mechanism of Chemokine Receptor CCR5 Involves Common Structural Changes but A Different Network of Interhelical Interactions Relative to Rhodopsin", *Cellular Signalling*, Vol. 19, pp. 1446–1456, 2007.

58. Nussinov, R. and C. J. Tsai, "Allostery in Disease and in Drug Discovery", *Cell*, Vol. 153, pp. 293–305, 2013.

59. Guo, J. and H.-X. Zhou, "Protein Allostery and Conformational Dynamics", *Chemical Reviews*, Vol. 116, pp. 6503–6515, 2016.

60. Nussinov, R. and C.-J. Tsai, "The Design of Covalent Allosteric Drugs", *Annual Review of Pharmacology and Toxicology*, Vol. 55, pp. 249–267, 2015.

61. Monod, J., J. P. Changeux and F. Jacob, "Allosteric Proteins and Cellular Control Systems", *Journal of Molecular Biology*, Vol. 6, pp. 306–329, 1963.

62. Lu, S., S. Li and J. Zhang, "Harnessing Allostery: A Novel Approach to Drug Discovery", *Medicinal Research Reviews*, Vol. 34, pp. 1242–1285, 2014.

63. Wodak, S. J., E. Paci, N. V. Dokholyan, I. N. Berezovsky, A. Horovitz, J. Li, V. J. Hilser, I. Bahar, J. Karanicolas, G. Stock, P. Hamm, R. H. Stote, J. Eberhardt, Y. Chebaro, A. Dejaegere, M. Cecchini, J. P. Changeux, P. G. Bolhuis, J. Vreede, P. Faccioli, S. Orioli, R. Ravasio, L. Yan, C. Brito, M. Wyart, P. Gkeka, I. Rivalta, G. Palermo, J. A. McCammon, J. Panecka-Hofman, R. C. Wade, A. D. Pizio, M. Y. Niv, R. Nussinov, C. J. Tsai, H. Jang, D. Padhorny, D. Kozakov and T. McLeish, "Allostery in Its Many Disguises: From Theory to Applications", *Structure*, Vol. 27, pp. 566–578, 2019.

64. Liu, J. and R. Nussinov, "Allostery: An Overview of Its History, Concepts, Methods, and Applications", *PLoS Comput. Biol.*, Vol. 12, p. e1004966, 2016.

65. Fleetwood, O., P. Matricon, J. Carlsson and L. Delemotte, "Energy Landscapes Reveal Agonist Control of G Protein-Coupled Receptor Activation via

Microswitches", *Biochemistry*, Vol. 59, pp. 880–891, 2020.

66. Jensen, A. A. and T. A. Spalding, "Allosteric Modulation of G-Protein Coupled Receptors", *European Journal of Pharmaceutical Sciences*, Vol. 21, pp. 407–420, 2004.

67. Bindslev, N., "Allosteric Transition: A Comparison of Two Models", *BMC Pharmacology and Toxicology*, Vol. 14, pp. 1–12, 2013.

68. Hall, D. A., "Modeling the Functional Effects of Allosteric Modulators at Pharmacological Receptors: An Extension of the Two-State Model of Receptor Activation", *Molecular Pharmacology*, Vol. 58, pp. 1412–1423, 2000.

69. May, L. T., K. Leach, P. M. Sexton and A. Christopoulos, "Allosteric Modulation of G Protein-Coupled Receptors", *Annual Review of Pharmacology and Toxicology*, Vol. 47, pp. 1–51, 2007.

70. Black, J. W. and P. Leff, "Operational Models of Pharmacological Agonism", *Proceedings of the Royal Society of London. Series B, Biological Sciences*, Vol. 220, pp. 141–162, 1983.

71. Kenakin, T., "Principles: Receptor Theory in Pharmacology", *Trends in Pharmacological Sciences*, Vol. 25, pp. 186–192, 2004.

72. Jakubík, J., A. Randáková, N. Chetverikov, E. E. El-Fakahany and V. Doležal, "The Operational Model of Allosteric Modulation of Pharmacological Agonism", *Scientific*, Vol. 10, pp. 1–20, 2020.

73. Gregory, K. J., J. Giraldo, J. Diao, A. Christopoulos and K. Leach, "Evaluation of Operational Models of Agonism and Allosterism at Receptors With Multiple Orthosteric Binding Sites", *Molecular Pharmacology*, Vol. 97, pp. 35–47, 2020.

74. Wenthur, C. J., P. R. Gentry, T. P. Mathews and C. W. Lindsley, "Drugs for Allosteric Sites on Receptors", *Annual Review of Pharmacology and Toxicology*,

Vol. 54, pp. 165–184, 2014.

75. Liu, L., Z. Fan, X. Rovira, L. Xue, S. Roux, I. Brabet, M. Xin, J.-P. Pin, P. Rondard and J. Liu, "Allosteric Ligands Control the Activation of A Class C GPCR Heterodimer by Acting at the Transmembrane Interface", *eLife*, Vol. 10, p. e70188, 2021.

76. Valant, C., J. R. Lane, P. M. Sexton and A. Christopoulos, "The Best of Both Worlds? Bitopic Orthosteric/Allosteric Ligands of G Protein-Coupled Receptors", *Annual Review of Pharmacology and Toxicology*, Vol. 52, pp. 153–178, 2012.

77. Slosky, L. M., M. G. Caron and L. S. Barak, "Biased Allosteric Modulators: New Frontiers in GPCR Drug Discovery", *Trends in Pharmacological Sciences*, Vol. 42, pp. 283–299, 2021.

78. Kenakin, T. P., "Ligand Detection in the Allosteric World", *Journal of Biomolecular Screening*, Vol. 15, pp. 119–130, 2010.

79. Keov, P., P. M. Sexton and A. Christopoulos, "Allosteric Modulation of G Protein-Coupled Receptors: A Pharmacological Perspective", *Neuropharmacology*, Vol. 60, pp. 24–35, 2011.

80. Christopoulos, A., L. T. May, V. A. Avlani and P. M. Sexton, "G-Protein-Coupled Receptor Allosterism: The Promise and the Problem(s)", *Biochemical Society Transactions*, Vol. 7, pp. 819–821, 2004.

81. Kenakin, T., "Biased Signaling as Allosteric Probe Dependence", *Cellular Signalling*, Vol. 79, p. 109844, 2021.

82. Valant, C., C. C. Felder, P. M. Sexton and A. Christopoulos, "Probe Dependence in the Allosteric Modulation of A G Protein-Coupled Receptor: Implications for Detection and Validation of Allosteric Ligand Effects", *Molecular Pharmacology*, Vol. 81, pp. 41–52, 2012.

83. Suratman, S., K. Leach, P. Sexton, C. Felder, R. Loiacono and A. Christopoulos, "Impact of Species Variability and 'Probe-Dependence' on the Detection and in vivo Validation of Allosteric Modulation at the M4 Muscarinic Acetylcholine Receptor", *British Journal of Pharmacology*, Vol. 162, pp. 1659–1670, 2011.

84. Wootten, D., A. Christopoulos and P. M. Sexton, "Emerging Paradigms in GPCR Allostery: Implications for Drug Discovery", *Nature Reviews Drug Discovery*, Vol. 12, pp. 630–644, 2013.

85. Sanchez-Soto, M., R. K. Verma, B. K. Willette, E. C. Gonye, A. M. Moore, A. E. Moritz, C. A. Boateng, H. Yano, R. B. Free, L. Shi and D. R. Sibley, "A Structural Basis for How Ligand Binding Site Changes Can Allosterically Regulate GPCR Signaling and Engender Functional Selectivity", *Science Signaling*, Vol. 13, 2020.

86. Langmead, C. J. and A. Christopoulos, "Functional and Structural Perspectives on Allosteric Modulation of GPCRs", *Current Opinion in Cell Biology*, Vol. 27, pp. 94–101, 2014.

87. Bologna, Z., J. P. Teoh, A. S. Bayoumi, Y. Tang and I. M. Kim, "Biased G Protein-Coupled Receptor Signaling: New Player in Modulating Physiology and Pathology", *Biomolecules and Therapeutics*, Vol. 25, pp. 12–25, 2017.

88. Wingler, L. M., M. A. Skiba, C. McMahon, D. P. Staus, A. L. Kleinhenz, C. M. Suomivuori, N. R. Latorraca, R. O. Dror, R. J. Lefkowitz and A. C. Kruse, "Angiotensin and Biased Analogs Induce Structurally Distinct Active Conformations Within A GPCR", *Science*, Vol. 367, pp. 888–892, 2020.

89. Slosky, L. M., Y. Bai, K. Toth, C. Ray, L. K. Rochelle, A. Badea, R. Chandrasekhar, V. M. Pogorelov, D. M. Abraham, N. Atluri, S. Peddibhotla, M. P. Hedrick, P. Hershberger, P. Maloney, H. Yuan, Z. Li, W. C. Wetsel, A. B. Pinkerton, L. S. Barak and M. G. Caron, "β-Arrestin-Biased Allosteric Modulator of NTSR1 Selectively Attenuates Addictive Behaviors", *Cell*, Vol. 181, pp. 1364–1379.e14, 2020.

90. Mitchell, M. ., "Mu-Opioid Receptor Biased Ligands: A Safer and Painless Discovery of Analgesics?", *Physiology & Behavior*, Vol. 176, pp. 139–148, 2016.

91. Stewart, G. D., L. Comps-Agrar, L. B. Nørskov-Lauritsen, J. P. Pin and J. Kniazeff, "Allosteric Interactions Between GABAB1 Subunits Control Orthosteric Binding Sites Occupancy Within GABAB Oligomers", *Neuropharmacology*, Vol. 136, pp. 92–101, 2018.

92. Harikumar, K. G., D. Wootten, D. I. Pinon, C. Koole, A. M. Ball, S. G. Furness, B. Graham, M. Dong, A. Christopoulos, L. J. Miller and P. M. Sexton, "Glucagon-Like Peptide-1 Receptor Dimerization Differentially Regulates Agonist Signaling but Does Not Affect Small Molecule Allostery", *Proceedings of the National Academy of Sciences of the United States of America*, Vol. 109, pp. 18607–18612, 2012.

93. Redka, D. S., T. Morizumi, G. Elmslie, P. Paranthaman, R. V. Shivnaraine, J. Ellis, O. P. Ernst and J. W. Wells, "Coupling of G Proteins to Reconstituted Monomers and Tetramers of the M2 Muscarinic Receptor", *Journal of Biological Chemistry*, Vol. 289, pp. 24347–24365, 2014.

94. Lane, J. R., P. Donthamsetti, J. Shonberg, C. J. Draper-Joyce, S. Dentry, M. Michino, L. Shi, L. Lopez, P. J. Scammells, B. Capuano, P. M. Sexton, J. A. Javitch and A. Christopoulos, "A New Mechanism of Allostery in A G Protein-Coupled Receptor Dimer", *Nature Chemical Biology 2014*, Vol. 10, pp. 745–752, 2014.

95. Shivnaraine, R. V., B. Kelly, K. S. Sankar, D. S. Redka, Y. R. Han, F. Huang, G. Elmslie, D. Pinto, Y. Li, J. V. Rocheleau, C. C. Gradinaru, J. Ellis and J. W. Wells, "Allosteric Modulation in Monomers and Oligomers of A G Protein-Coupled Receptor", *eLife*, Vol. 5, 2016.

96. Wagner, J., T. Sungkaworn, K. G. Heinze, M. J. Lohse and D. Calebiro, *GPCRs in Drug Discovery*, Vol. 1335, Humana New York, NY, 2015.

97. Vroling, B., M. Sanders, C. Baakman, A. Borrmann, S. Verhoeven, J. Klomp, L. Oliveira, J. D. Vlieg and G. Vriend, "GPCRDB: Information System for G Protein-Coupled Receptors", *Nucleic Acids Research*, Vol. 39, pp. D309–D319, 2011.

98. Congreve, M., C. Langmead and F. H. Marshall, *The Use of GPCR Structures in Drug Design*, Vol. 62, Elsevier Inc., 2011.

99. Andrews, S. P., G. A. Brown and J. A. Christopher, "Structure-Based and Fragment-Based GPCR Drug Discovery", *ChemMedChem*, Vol. 9, pp. 256–275, 2014.

100. Congreve, M., C. Oswald and F. H. Marshall, "Applying Structure-Based Drug Design Approaches to Allosteric Modulators of GPCRs", *Trends in Pharmacological Sciences*, Vol. 38, pp. 837–847, 2017.

101. Chan, H. S., Y. Li, T. Dahoun, H. Vogel and S. Yuan, "New Binding Sites, New Opportunities for GPCR Drug Discovery", *Trends in Biochemical Sciences*, Vol. 44, pp. 312–330, 2019.

102. Schoepfer, J., W. Jahnke, G. Berellini, S. Buonamici, S. Cotesta, S. W. Cowan-Jacob, S. Dodd, P. Drueckes, D. Fabbro, T. Gabriel, J.-M. Groell, R. M. Grotzfeld, A. Q. Hassan, C. Henry, V. Iyer, D. Jones, F. Lombardo, A. Loo, P. W. Manley, X. Pellé, G. Rummel, B. Salem, M. Warmuth, A. A. Wylie, T. Zoller, A. L. Marzinzik and P. Furet, "Discovery of Asciminib (ABL001), An Allosteric Inhibitor of the Tyrosine Kinase Activity of BCR-ABL1", *Journal of Medicinal Chemistry*, Vol. 61, pp. 8120–8135, 2018.

103. Kliewer, A., F. Schmiedel, S. Sianati, A. Bailey, J. T. Bateman, E. S. Levitt, J. T. Williams, M. J. Christie and S. Schulz, "Phosphorylation-Deficient G-Protein-Biased μ-Opioid Receptors Improve Analgesia and Diminish Tolerance but Worsen Opioid Side Effects", *Nature Communications*, Vol. 10, 2019.

104. Lu, S., X. He, D. Ni and J. Zhang, "Allosteric Modulator Discovery: From Serendipity to Structure-Based Design", *Journal of Medicinal Chemistry*, Vol. 62, pp. 6405–6421, 2019.

105. Bartuzi, D., A. A. Kaczor and D. Matosiuk, "Signaling Within Allosteric Machines: Signal Transmission Pathways Inside G Protein-Coupled Receptors", *Molecules 2017, Vol. 22, Page 1188*, Vol. 22, p. 1188, 2017.

106. Bartuzi, D., A. A. Kaczor and D. Matosiuk, "Interplay between Two Allosteric Sites and Their Influence on Agonist Binding in Human μ Opioid Receptor", *Journal of Chemical Information and Modeling*, Vol. 56, pp. 563–570, 2016.

107. Żuk, J., D. Bartuzi, A. G. Silva, M. Pitucha, O. Koszła, T. M. Wróbel, D. Matosiuk, M. Castro and A. A. Kaczor, "Allosteric Modulation of Dopamine D2L Receptor in Complex With GI1 and GI2 Proteins: The Effect of Subtle Structural and Stereochemical Ligand Modifications", *Pharmacological Reports*, Vol. 74, pp. 406–424, 2022.

108. White, K. L., M. T. Eddy, Z.-G. Gao, G. W. Han, T. Lian, A. Deary, N. Patel, K. A. Jacobson, V. Katritch and R. C. Stevens, "Structural Connection between Activation Microswitch and Allosteric Sodium Site in GPCR Signaling", *Structure*, Vol. 26, pp. 259–269.e5, 2018.

109. Wang, Y., Z. Yu, W. Xiao, S. Lu and J. Zhang, "Allosteric Binding Sites at the Receptor-Lipid Bilayer Interface: Novel Targets for GPCR Drug Discovery", *Drug Discovery Today*, pp. 690–703, 2020.

110. Bartuzi, D., A. A. Kaczor and D. Matosiuk, *Opportunities and Challenges in the Discovery of Allosteric Modulators of GPCRs*, Vol. 1705, Humana Press Inc., 2018.

111. Tee, W.-V., E. Guarnera and I. N. Berezovsky, "Reversing Allosteric Communication: From Detecting Allosteric Sites to Inducing and Tuning Targeted Allosteric

Response", *PLoS Computational Biology*, Vol. 14, p. e1006228, 2018.

112. Koehl, A., H. Hu, S. Maeda, Y. Zhang, Q. Qu, J. M. Paggi, N. R. Latorraca, D. Hilger, R. Dawson, H. Matile, G. F. X. Schertler, S. Granier, W. I. Weis, R. O. Dror, A. Manglik, G. Skiniotis and B. K. Kobilka, "Structure of the μ-Opioid Receptor-Gi Protein Complex", *Nature*, Vol. 558, pp. 547–552, 2018.

113. Conner, A. C., J. Barwell, D. R. Poyner and M. Wheatley, *The Use of Site-Directed Mutagenesis to Study GPCRs*, pp. 85–98, Humana Press, Totowa, NJ, 2011.

114. Guo, H., S. An, R. Ward, Y. Yang, Y. Liu, X. X. Guo, Q. Hao and T. R. Xu, "Methods Used to Study the Oligomeric Structure of G-Protein-Coupled Receptors", *Bioscience Reports*, Vol. 37, pp. 1–20, 2017.

115. Lismont, E., L. Verbakel, E. Vogel, J. Corbisier, G. N. Degroot, R. Verdonck, H. Verlinden, E. Marchal, J. Y. Springael and J. V. Broeck, "Can BRET-Based Biosensors Be Used to Characterize G-protein Mediated Signaling Pathways of An Insect GPCR, the Schistocerca gregaria Crf-Related Diuretic Hormone Receptor?", *Insect Biochemistry and Molecular Biology*, Vol. 122, p. 103392, 2020.

116. Vasudevan, N. T., *cAMP Assays in GPCR Drug Discovery*, Vol. 142, Academic Press Inc., 2017.

117. Lee, M. M. V. D., M. Bras, C. J. V. Koppen and G. J. Zaman, "β-Arrestin Recruitment Assay for the Identification of Agonists of the Sphingosine 1-Phosphate Receptor EDG1", *Journal of Biomolecular Screening*, Vol. 13, pp. 986–998, 2008.

118. Lauwers, E., B. Landuyt, L. Arckens, L. Schoofs and W. Luyten, "Obestatin Does Not Activate Orphan G Protein-Coupled Receptor GPR39", *Biochemical and Biophysical Research Communications*, Vol. 351, pp. 21–25, 2006.

119. Dogra, S., C. Sona, A. Kumar and P. N. Yadav, "Chapter 12-Tango Assay for

Ligand-Induced GPCR-β-Arrestin2 Interaction: Application in Drug Discovery", A. K. Shukla (Editor), *G Protein-Coupled Receptors*, Vol. 132 of *Methods in Cell Biology*, pp. 233–254, Academic Press, 2016.

120. Liu, X., S. Lu, K. Song, Q. Shen, D. Ni, Q. Li, X. He, H. Zhang, Q. Wang, Y. Chen, X. Li, J. Wu, C. Sheng, G. Chen, Y. Liu, X. Lu and J. Zhang, "Unraveling Allosteric Landscapes of Allosterome With ASD", *Nucleic Acids Research*, Vol. 48, pp. D394–D401, 2019.

121. Huang, W., G. Wang, Q. Shen, X. Liu, S. Lu, L. Geng, Z. Huang and J. Zhang, "ASBench: Benchmarking Sets for Allosteric Discovery", *Bioinformatics*, Vol. 31, pp. 2598–2600, 2015.

122. Hedderich, J. B., M. Persechino, K. Becker, F. M. Heydenreich, T. Gutermuth, M. Bouvier, M. Bünemann and P. Kolb, "The Pocketome of G-Protein-Coupled Receptors Reveals Previously Untargeted Allosteric Sites", *Nature Communications*, Vol. 13, p. 2567, 2022.

123. Kling, R. C., C. Burchardt, J. Einsiedel, H. Hübner and P. Gmeiner, "Structure-Based Exploration of An Allosteric Binding Pocket in the NTS1 Receptor Using Bitopic NT(8-13) Derivatives and Molecular Dynamics Simulations", *Journal of Molecular Modeling*, Vol. 25, pp. 2–11, 2019.

124. Noha, S. M., H. Schmidhammer and M. Spetea, "Molecular Docking, Molecular Dynamics, and Structure-Activity Relationship Explorations of 14-Oxygenated N-Methylmorphinan-6-ones as Potent μ-Opioid Receptor Agonists", *ACS Chemical Neuroscience*, Vol. 8, pp. 1327–1337, 2017.

125. Payghan, P. V., I. Bera, D. Bhattacharyya and N. Ghoshal, "Computational Studies for Structure-Based Drug Designing Against Transmembrane Receptors: pLGICs and Class A GPCRs", *Frontiers in Physics*, Vol. 6, 2018.

126. Ballante, F., A. J. Kooistra, S. Kampen, C. de Graaf and J. Carlsson, "Structure-

Based Virtual Screening for Ligands of G Protein–Coupled Receptors: What Can Molecular Docking Do for You?", *Pharmacological Reviews*, Vol. 73, pp. 527–656, 2021.

127. Hospital, A., J. R. Goñi, M. Orozco and J. L. Gelpí, "Molecular Dynamics Simulations: Advances and Applications", *Advances and Applications in Bioinformatics and Chemistry*, Vol. 8, pp. 37–47, 2015.

128. Metcalf, R. L. and W. H. Luckmann, *Introduction to Insect Pest Management*, J. Wiley and Sons, Wiley-interscience publ., 3 edn., 1994.

129. Casida, J. E. and K. A. Durkin, "Pesticide Chemical Research in Toxicology: Lessons from Nature", *Chemical Research in Toxicology*, Vol. 30, pp. 94–104, 2017.

130. Casida, J. E., "Pest Toxicology: The Primary Mechanisms of Pesticide Action", *Chemical Research in Toxicology*, Vol. 22, pp. 609–619, 2009.

131. Casida, J. E. and S. Spring, "The Greening of Pesticide-Environment Interactions: Some Personal Observations", *Environ Health Perspect*, Vol. 120, pp. 487–493, 2012.

132. Maksymiv, I., "70 Pesticides: Benefits and Hazards", *Journal of Vasyl Stefanyk Precarpathian National University*, Vol. 2, pp. 70–76, 2015.

133. Ã, J. C. and H. Dobson, "The Benefits of Pesticides to Mankind and the Environment", *Crop Protection*, Vol. 26, pp. 1337–1348, 2007.

134. Hill, C. A., J. M. Meyer, K. F. Ejendal, D. F. Echeverry, E. G. Lang, L. V. Avramova, J. M. Conley and V. J. Watts, "Re-Invigorating the Insecticide Discovery Pipeline for Vector Control: GPCRs as Targets for the Identification of Next Gen Insecticides", *Pesticide Biochemistry and Physiology*, Vol. 106, pp. 141–148, 2013.

135. Aktar, W., D. Sengupta and A. Chowdhury, "Impact of Pesticides Use in Agriculture : Their Benefits and Hazards", *Interdisciplinary Toxicology*, Vol. 2, pp. 1–12, 2009.

136. Damalas, C. A., "Pesticides in Agriculture: Environmental and Health Risks", *Current Opinion in Environmental Science and Health*, Vol. 4, pp. 4–5, 2018.

137. Mousavi-Avval, S. H. and A. Shah, "Techno-Economic Analysis of Pennycress Production, Harvest and Post-harvest Logistics for Renewable Jet Fuel", *Renewable and Sustainable Energy Reviews*, Vol. 123, 2020.

138. Clasen, B., V. L. Loro, C. R. Murussi, T. L. Tiecher, B. Moraes and R. Zanella, "Bioaccumulation and Oxidative Stress Caused by Pesticides in Cyprinus Carpio Reared in A Rice-Fish System", *Science of the Total Environment*, Vol. 626, pp. 737–743, 2018.

139. Sancho, E., M. Ferrando, C. Lleó and E. Andreu-Moliner, "Pesticide Toxicokinetics in Fish: Accumulation and Elimination", *Ecotoxicology and Environmental Safety*, Vol. 41, pp. 245–250, 1998.

140. Pucher, J., T. Gut, R. Mayrhofer, M. El-Matbouli, P. H. Viet, N. T. Ngoc, M. Lamers, T. Streck and U. Focken, "Pesticide-Contaminated Feeds in Integrated Grass Carp Aquaculture: Toxicology and Bioaccumulation", *Diseases of Aquatic Organisms*, Vol. 108, pp. 137–147, 2014.

141. Katagi, T., *Metabolism of Pesticides in Aquatic Organisms and Metabolism of Pesticides*, Vol. 204, Springer New York, 2010.

142. Bolognesi, C. and F. Merlo, "Pesticides : Human Health Effects", *Elsevier*, pp. 438–453, 2011.

143. Kim, K.-H. H., E. Kabir and S. A. Jahan, "Exposure to Pesticides and the Associated Human Health Effects", *Science of the Total Environment*, Vol. 575, pp.

525–535, 2017.

144. Prado, J. B., P. R. Mulay, E. J. Kasner, H. K. Bojes and G. M. Calvert, "Acute Pesticide-Related Illness Among Farmworkers: Barriers to Reporting to Public Health Authorities", *Journal of Agromedicine*, Vol. 22, pp. 395–405, 2017.

145. Eskenazi, B., L. G. Rosas, A. R. Marks, A. Bradman, K. Harley, N. Holland, C. Johnson, L. Fenster and D. B. Barr, "Pesticide Toxicity and the Developing Brain", *Basic and Clinical Pharmacology and Toxicology*, Vol. 102, pp. 228–236, 2008.

146. Nataraj, B., D. Hemalatha, B. Rangasamy, K. Maharajan and M. Ramesh, "Hepatic Oxidative Stress, Genotoxicity and Histopathological Alteration in Fresh Water Fish Labeo Rohita Exposed to Organophosphorus Pesticide Profenofos", *Biocatalysis and Agricultural Biotechnology*, Vol. 12, pp. 185–190, 2017.

147. Mahapatra, K., S. De, S. Banerjee and S. Roy, "Pesticide Mediated Oxidative Stress Induces Genotoxicity and Disrupts Chromatin Structure in Fenugreek (Trigonella foenum - Graecum l.) Seedlings", *Journal of Hazardous Materials*, Vol. 369, pp. 362–374, 2019.

148. Odetti, L. M., E. C. L. González, M. L. Romito, M. F. Simoniello and G. L. Poletta, "Genotoxicity and Oxidative Stress in Caiman Latirostris Hatchlings Exposed to Pesticide Formulations and Their Mixtures During Incubation Period", *Ecotoxicology and Environmental Safety*, Vol. 193, p. 110312, 2020.

149. González, E. C. L., P. A. Siroski and G. L. Poletta, "Genotoxicity Induced by Widely Used Pesticide Binary Mixtures on Caiman Latirostris (Broad-Snouted Caiman)", *Chemosphere*, Vol. 232, pp. 337–344, 2019.

150. Greim, H., D. Saltmiras, V. Mostert and C. Strupp, "Evaluation of Carcinogenic Potential of the Herbicide Glyphosate, Drawing on Tumor Incidence Data From Fourteen Chronic/Carcinogenicity Rodent Studies", *Critical Reviews in Toxicol-*

ogy, Vol. 45, pp. 185–208, 2015.

151. Davoren, M. J. and R. H. Schiestl, "Glyphosate-based Herbicides and Cancer Risk: A Post-IARC Decision Review of Potential Mechanisms, Policy and Avenues of Research", *Carcinogenesis*, Vol. 39, pp. 1207–1215, 2018.

152. Khan, M. A., Z. Khan, W. Ahmad, B. Paul, S. Paul, C. Aggarwal and M. S. Akhtar, *Insect Pest Resistance: An Alternative Approach for Crop Protection*, Springer International Publishing, 2015.

153. Li, T., L. Liu, L. Zhang and N. Liu, "Role of G-Protein-Coupled Receptor-Related Genes in Insecticide Resistance of the Mosquito, Culex quinquefasciatus", *Scientific Reports*, Vol. 4, p. 6474, 2014.

154. Ma, Z., Y. Zhang, C. You, X. Zeng and X. Gao, "The Role of G Protein-Coupled Receptor-Related Genes in Cytochrome P450-Mediated Resistance of the House Fly, Musca domestica (Diptera: Muscidae), to Imidacloprid", *Insect Molecular Biology*, Vol. 29, pp. 92–103, 2020.

155. Swale, D. R., "Perspectives on New Strategies for the Identification and Development of Insecticide Targets", *Pesticide Biochemistry and Physiology*, Vol. 161, pp. 23–32, 2019.

156. Keswani, C., H. B. Singh, C. García-Estrada, J. Caradus, Y. W. He, S. Mezaache-Aichour, T. R. Glare, R. Borriss and E. Sansinenea, "Antimicrobial Secondary Metabolites From Agriculturally Important Bacteria as Next-Generation Pesticides", *Applied Microbiology and Biotechnology*, Vol. 104, pp. 1013–1034, 2020.

157. Domínguez-Arrizabalaga, M., M. Villanueva, B. Escriche, C. Ancín-Azpilicueta and P. Caballero, "Insecticidal Activity of Bacillus thuringiensis Proteins Against Coleopteran Pests", *Toxins*, Vol. 12, p. 430, 2020.

158. Fierascu, R. C., I. C. I. Fierascu, C. E. Dinu-Pirvu, I. C. I. Fierascu and

A. Paunescu, "The Application of Essential Oils as A Next-Generation of Pesticides: Recent Developments and Future Perspectives", *Zeitschrift fur Naturforschung - Section C Journal of Biosciences*, Vol. 75, pp. 183–204, 2020.

159. Jain, P. K., R. Bhattacharya, D. Kohli, R. Aminedi and P. K. Agrawal, *RNAi for Resistance Against Biotic Stresses in Crop Plants*, Springer International Publishing, 2018.

160. Bai, H., F. Zhu, K. Shah and S. R. Palli, "Large-Scale RNAi Screen of G Protein-Coupled Receptors Involved in Larval Growth, Molting and Metamorphosis in the Red Flour Beetle", *BMC Genomics*, Vol. 12, p. 388, 2011.

161. Zhu, K. Y. and S. R. Palli, "Mechanisms, Applications, and Challenges of Insect RNA Interference", *Annual Review of Entomology*, Vol. 65, pp. 293–311, 2020.

162. Riddiford, L. M. and M. Ashburner, "Effects of Juvenile Hormone Mimics on Larval Development and Metamorphosis of Drosophila Melanogaster", *General and Comparative Endocrinology*, Vol. 82, pp. 172–183, 1991.

163. Dhadialla, T. S., G. R. Carlson and D. P. Le, "New Insecticides With Ecdysteroidal and Juvenile Hormone Activity", *Annual Review of Entomology*, Vol. 43, pp. 545–569, 1998.

164. Restifo, L. L. and T. G. Wilson, "A Juvenile Hormone Agonist Reveals Distinct Developmental Pathways Mediated by Ecdysone-Inducible Broad Complex Transcription Factors", *Developmental Genetics*, Vol. 22, pp. 141–159, 1998.

165. Syed, T., M. Askari, Z. Meng, Y. Li, M. A. Abid, Y. Wei, S. Guo, C. Liang and R. Zhang, "Current Insights on Vegetative Insecticidal Proteins (Vip) as Next Generation Pest Killers", *Toxins*, Vol. 12, p. 522, 2020.

166. Bai, H. and S. R. Palli, *G Protein-Coupled Receptors as Target Sites for Insecticide Discovery*, Springer Netherlands, 2013.

167. Enan, E., "Insecticidal Activity of Essential Oils: Octopaminergic Sites of Action", *Comparative Biochemistry and Physiology-C Toxicology and Pharmacology*, Vol. 130, pp. 325–337, 2001.

168. Ahmed, M. A. I. and C. F. A. Vogel, "The Synergistic Effect of Octopamine Receptor Agonists on Selected Insect Growth Regulators on Culex quinquefasciatus Say (Diptera: Culicidae) Mosquitoes", *One Health*, Vol. 10, p. 100138, 2020.

169. Ahmed, M. A. I. and C. F. A. Vogel, "The Role of Octopamine Receptor Agonists in the Synergistic Toxicity of Certain Insect Growth Regulators (IGRs) In Controlling Dengue Vector Aedes Aegypti (Diptera: Culicidae) Mosquito", *Acta Tropica*, Vol. 155, pp. 1–5, 2016.

170. Pino, J. D., P. V. Moyano-Cires, M. J. Anadon, M. J. Díaz, M. Lobo, M. A. Capo and M. T. Frejo, "Molecular Mechanisms of Amitraz Mammalian Toxicity: A Comprehensive Review of Existing Data", *Chemical Research in Toxicology*, Vol. 28, pp. 1073–1094, 2015.

171. Leung, V. K. S., T. Y. K. Chan and V. T. F. Yeung, "Amitraz Poisioning in Humans", *Clinical Toxicology*, 1999.

172. Rajabi, H., J. Wu and S. Gorb, "Insects: Functional Morphology, Biomechanics and Biomimetics", *Insects*, Vol. 12, p. 1108, 2021.

173. Nijhout, H., *Insect Hormones*, Princeton University Press, 1994.

174. Li, F., X. Zhao, M. Li, K. He, C. Huang, Y. Zhou, Z. Li and J. R. Walters, "Insect Genomes: Progress and Challenges", *Insect Molecular Biology*, Vol. 28, pp. 739–758, 2019.

175. Mayhew, P. J., "Why Are There So Many Insect Species? Perspectives From Fossils and Phylogenies", *Biological Reviews*, Vol. 82, pp. 425–454, 2007.

176. Berardi, L., M. Pivato, G. Arrigoni, E. Mitali, A. R. Trentin, M. Olivieri,

C. Kerdelhué, F. Dorkeld, S. Nidelet, E. Dubois, A. Battisti and A. Masi, "Proteome Analysis of Urticating Setae From Thaumetopoea pityocampa (Lepidoptera: Notodontidae)", *Journal of Medical Entomology*, Vol. 54, pp. 1560–1566, 2017.

177. Bonamonte, D., C. Foti, M. Vestita and G. Angelini, "Skin Reactions to Pine Processionary Caterpillar Thaumetopoea pityocampa Schiff", *The Scientific World Journal*, Vol. 2013, pp. 1–6, 2013.

178. Avtzis, D. N., D. Petsopoulos, G. I. Memtsas, N. G. Kavallieratos, C. G. Athanassiou, M. C. Boukouvala and T. Schowalter, "Revisiting the Distribution of Thaumetopoea pityocampa (Lepidoptera: Notodontidae) and T. pityocampa Ena Clade in Greece", *Journal of Economic Entomology*, Vol. 111, pp. 1256–1260, 2018.

179. Trematerra, P., M. Colacci, C. G. Athanassiou, N. G. Kavallieratos, C. I. Rumbos, M. C. Boukouvala, A. J. Nikolaidou, D. C. Kontodimas, E. Benavent-Fernández and S. Gálvez-Settier, "Evaluation of Mating Disruption for the Control of Thaumetopoea pityocampa (Lepidoptera: Thaumetopoeidae) in Suburban Recreational Areas in Italy and Greece", *Journal of Economic Entomology*, Vol. 112, pp. 2229–2235, 2019.

180. Kaszak, I., M. Planellas and B. Dworecka-Kaszak, "Pine Processionary Caterpillar, Thaumetopoea pityocampa Denis and Schiffermüller, 1775 Contact as A Health Risk for Dogs", *Annals of Parasitology*, Vol. 61, pp. 159–163, 2015.

181. Bruchim, Y., E. Ranen, J. Saragusty and I. Aroch, "Severe Tongue Necrosis Associated With Pine Processionary Moth (Thaumetopoea Wilkinsoni) Ingestion in Three Dogs", *Toxicon: Official Journal of the International Society on Toxinology*, Vol. 45, pp. 443–447, 2005.

182. Berardi, L., A. Battisti and E. Negrisolo, "The Allergenic Protein Tha P2 of Processionary Moths of the Genus Thaumetopoea (Thaumetopoeinae, Notodontidae,

Lepidoptera): Characterization and Evolution", *Gene*, Vol. 574, pp. 317–324, 2015.

183. Avtzis, D. N., M. Schebeck, D. Petsopoulos, G. I. Memtsas, C. Stauffer, N. G. Kavallieratos, C. G. Athanassiou and M. C. Boukouvala, "New Data on the Range Expansion of the Thaumetopoea pityocampa (Lepidoptera: Notodontidae) 'ENA clade' in Greece: The Role of Bacterial Endosymbionts", *Journal of Economic Entomology*, Vol. 112, pp. 2761–2766, 2019.

184. Colacci, M., N. G. Kavallieratos, C. G. Athanassiou, M. C. Boukouvala, C. I. Rumbos, D. C. Kontodimas, D. Pardo, J. Sancho, E. Benavent-Fernández, S. Gálvez-Settier, A. Sciarretta and P. Trematerra, "Management of the Pine Processionary Moth, Thaumetopoea pityocampa (Lepidoptera: Thaumetopoeidae), in Urban and Suburban Areas: Trials With Trunk Barrier and Adhesive Barrier Trap Devices", *Journal of Economic Entomology*, Vol. 111, pp. 227–238, 2018.

185. Shahraki, A., A. Isbilir, B. Dogan, M. Lohse, S. Durdagi and N. Birgul-Iyison, "Structural and Functional Characterization of Allatostatin Receptor Type-C of Thaumetopoea pityocampa Revealed the Importance of Q271 6.55 Residue in G Protein-Dependent Activation Pathway", *Journal of Chemical Information and Modeling*, Vol. 3, pp. 1–27, 2020.

186. Shahraki, A., Y. Yu, Z. M. Gul, C. Liang and N. B. Iyison, "Whole Genome Sequencing of Thaumetopoea pityocampa Revealed Putative Pesticide Targets", *Genomics*, Vol. 112, pp. 4203–4207, 2020.

187. Harder, E., W. Damm, J. Maple, C. Wu, M. Reboul, J. Y. Xiang, L. Wang, D. Lupyan, M. K. Dahlgren, J. L. Knight, J. W. Kaus, D. S. Cerutti, G. Krilov, W. L. Jorgensen, R. Abel and R. A. Friesner, "OPLS3: A Force Field Providing Broad Coverage of Drug-like Small Molecules and Proteins", *Journal of Chemical Theory and Computation*, Vol. 12, pp. 281–296, 2016.

188. Huang, W., S. Lu, Z. Huang, X. Liu, L. Mou, Y. Luo, Y. Zhao, Y. Liu, Z. Chen, T. Hou and J. Zhang, "Allosite: A Method for Predicting Allosteric Sites", *Bioinformatics*, Vol. 29, pp. 2357–2359, 2013.

189. Panjkovich, A. and X. Daura, "PARS: A Web Server for the Prediction of Protein Allosteric and Regulatory Sites", *Bioinformatics (Oxford, England)*, Vol. 30, pp. 1314–1315, 2014.

190. Schmidtke, P., A. Bidon-Chanal, F. J. Luque and X. Barril, "MDpocket: Open-Source Cavity Detection and Characterization on Molecular Dynamics Trajectories", *Bioinformatics*, Vol. 27, pp. 3276–3285, 2011.

191. Humphrey, W., A. Dalke and K. Schulten, "VMD: Visual Molecular Dynamics", *Journal of Molecular Graphics*, Vol. 14, pp. 33–38, 1996.

192. Trott, O. and A. J. Olson, "Autodock Vina: Improving the Speed and Accuracy of Docking With A New Scoring Function, Efficient Optimization and Multithreading", *Journal of Computational Chemistry*, Vol. 31, p. 455, 2010.

193. Dallakyan, S. and A. J. Olson, "Small-Molecule Library Screening by Docking With PyRx", *Methods in Molecular Biology (Clifton, N.J.)*, Vol. 1263, pp. 243–250, 2015.

194. Lomize, M. A., I. D. Pogozheva, H. Joo, H. I. Mosberg and A. L. Lomize, "OPM Database and PPM Web Server: Resources for Positioning of Proteins in Membranes", *Nucleic Acids Research*, Vol. 40, pp. 370–376, 2012.

195. Carugo, O., "How Root-Mean-Square Distance (R.M.S.D.) Values Depend on the Resolution of Protein Structures That Are Compared", *Journal of Applied Crystallography*, Vol. 36, pp. 125–128, 2003.

196. Badaczewska-Dawid, A., A. Kolinski and S. Kmiecik, "Protocols for Fast Simulations of Protein Structure Flexibility Using Cabs-Flex and Surpass", *BioRxiv*,

2019.

197. Kirchmair, J., P. Markt, S. Distinto, G. Wolber and T. Langer, "Evaluation of the Performance of 3D Virtual Screening Protocols: RMSD Comparisons, Enrichment Assessments, and Decoy Selection-What Can We Learn From Earlier Mistakes?", *Journal of Computer-Aided Molecular Design*, Vol. 22, pp. 213–228, 2008.

198. Cooper, A., "Thermodynamic Fluctuations in Protein Molecules.", *Proceedings of the National Academy of Sciences*, Vol. 73, pp. 2740–2741, 1976.

199. Wang, H., Z. Gao, P. Song, B. Hu, J. Wang and M. Cheng, "Molecular Dynamics Simulation and QM/MM Calculation Reveal the Selectivity Mechanism of Type I 1/2 Kinase Inhibitors: The Effect of Intramolecular H-Bonds and Conformational Restriction for Improved Selectivity", *Physical Chemistry Chemical Physics*, Vol. 21, pp. 24147–24164, 2019.

200. Kuzmanic, A. and B. Zagrovic, "Determination of Ensemble-Average Pairwise Root Mean-Square Deviation from Experimental B-Factors", *Biophysical Journal*, Vol. 98, pp. 861–871, 2010.

201. Inoue, A., J. Ishiguro, H. Kitamura, N. Arima, M. Okutani, A. Shuto, S. Higashiyama, T. Ohwada, H. Arai, K. Makide and J. Aoki, "TGFα Shedding Assay: An Accurate and Versatile Method for Detecting GPCR Activation", *Nature Methods*, Vol. 9, pp. 1021–1029, 2012.

202. Dong, Y. Q., Z. Y. Wang and T. Z. Jing, "Functional Characterization of ASTC (Allatostatin C) and ASTCC (Allatostatin Double C) in Clostera anastomosis (Lepidoptera: Notodontidae)", *Gene*, Vol. 598, pp. 1–8, 2017.

203. Li, Y., S. Hernandez-Martinez and F. G. Noriega, "Inhibition of Juvenile Hormone Biosynthesis in Mosquitoes: Effect of Allatostatic Head Factors, PISCF- And YXFGL-Amide-Allatostatins", *Regulatory Peptides*, Vol. 118, pp. 175–182, 2004.

204. Lu, J., N. Byrne, J. Wang, G. Bricogne, F. K. Brown, H. R. Chobanian, S. L. Colletti, J. D. Salvo, B. Thomas-Fowlkes, Y. Guo, D. L. Hall, J. Hadix, N. B. Hastings, J. D. Hermes, T. Ho, A. D. Howard, H. Josien, M. Kornienko, K. J. Lumb, M. W. Miller, S. B. Patel, B. Pio, C. W. Plummer, B. S. Sherborne, P. Sheth, S. Souza, S. Tummala, C. Vonrhein, M. Webb, S. J. Allen, J. M. Johnston, A. B. Weinglass, S. Sharma and S. M. Soisson, "Structural Basis for the Cooperative Allosteric Activation of the Free Fatty Acid Receptor GPR40", *Nature Structural and Molecular Biology*, Vol. 24, pp. 570–577, 2017.

205. Xu, J., H. Hübner, Y. Hu and X. Niu, "An Allosteric Ligand Stabilizes Distinct Conformations in the M2 Muscarinic Acetylcholine Receptor", *bioRxiv*, pp. 1–24, 2021.

206. Liu, H., H. R. Kim, R. N. Deepak, L. Wang, K. Y. Chung, H. Fan, Z. Wei and C. Zhang, "Orthosteric and Allosteric Action of the C5a Receptor Antagonists", *Nature Structural and Molecular Biology*, Vol. 25, pp. 472–481, 2018.

207. Caliman, A. D., Y. Miao and J. A. McCammon, "Mapping the Allosteric Sites of the A2A Adenosine Receptor", *Chemical Biology & Drug Design*, Vol. 91, pp. 5–16, 2018.

208. Liu, X., A. Masoudi, A. W. Kahsai, L. yin Huang, B. Pani, D. P. Staus, P. J. Shim, K. Hirata, R. K. Simhal, A. M. Schwalb, P. K. Rambarat, S. Ahn, R. J. Lefkowitz and B. Kobilka, "Mechanism of β2AR Regulation by An Intracellular Positive Allosteric Modulator", *Science*, Vol. 364, pp. 1283–1287, 2019.

APPENDIX A: AMINO ACID ABBREVIATIONS

Table A.1. Amino acid names, abbreviations, and one-letter codes

Amino Acid	One-Letter Code	Three-Letter Code
Alanine	A	Ala
Arginine	R	Arg
Asparagine	N	Asn
Aspartic acid	D	Asp
Cysteine	C	Cys
Glutamine	Q	Gln
Glutamic acid	E	Glu
Glycine	G	Gly
Histidine	H	His
Isoleucine	I	Ile
Leucine	L	Leu
Lysine	K	Lys
Methionine	M	Met
Phenylalanine	F	Phe
Proline	P	Pro
Serine	S	Ser
Threonine	T	Thre
Tryptophan	W	Trp
Tyrosine	Y	Tyr
Valine	V	Val

APPENDIX B: AMINO ACID SEQUENCE OF ASTR-C

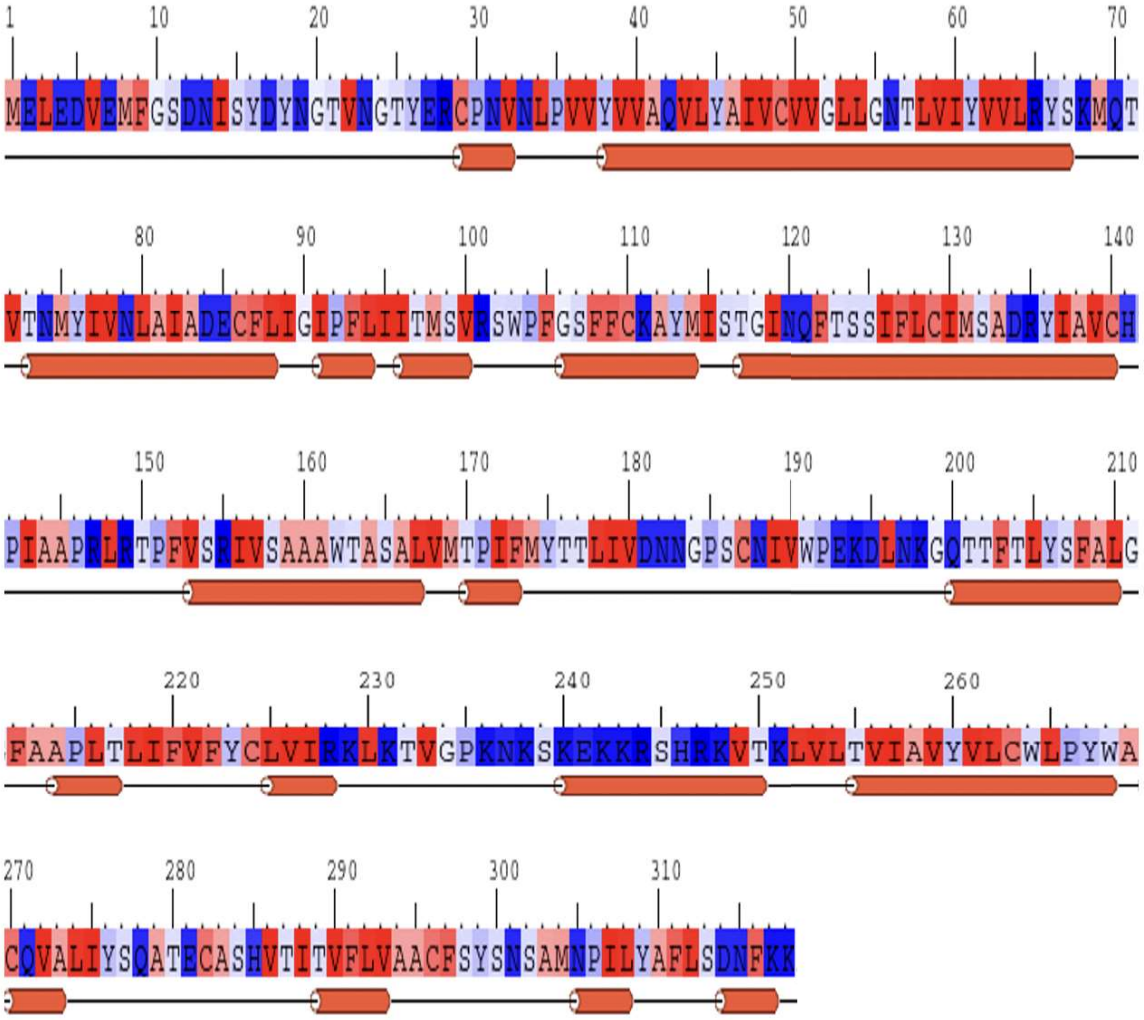

Figure B.1. Amino acid sequence of allatostatin receptor type-C.